

In Vitro Microfluidic Models for Neurodegenerative Disorders

Tatsuya Osaki, Yoojin Shin, Vivek Sivathanu, Marco Campisi, and Roger D. Kamm*

Microfluidic devices enable novel means of emulating neurodegenerative disease pathophysiology in vitro. These organ-on-a-chip systems can potentially reduce animal testing and substitute (or augment) simple 2D culture systems. Reconstituting critical features of neurodegenerative diseases in a biomimetic system using microfluidics can thereby accelerate drug discovery and improve our understanding of the mechanisms of several currently incurable diseases. This review describes latest advances in modeling neurodegenerative diseases in the central nervous system and the peripheral nervous system. First, this study summarizes fundamental advantages of microfluidic devices in the creation of compartmentalized cell culture microenvironments for the co-culture of neurons, glial cells, endothelial cells, and skeletal muscle cells and in their recapitulation of spatiotemporal chemical gradients and mechanical microenvironments. Then, this reviews neurodegenerative-disease-on-a-chip models focusing on Alzheimer's disease, Parkinson's disease, and amyotrophic lateral sclerosis. Finally, this study discusses about current drawbacks of these models and strategies that may overcome them. These organ-on-chip technologies can be useful to be the first line of testing line in drug development and toxicology studies, which can contribute significantly to minimize the phase of animal testing steps.

1. Introduction

Neurodegenerative diseases involve the progressive loss of neural cell function due to a variety of factors including oxidative stress and protein aggregation and misfolding in the central nervous system (CNS) and peripheral nervous system (PNS). The dysfunction and disruption of neuronal networks are triggered not only by cell death but also by alterations in

the cellular microenvironment and interactions between various cell types present: neurons, astrocytes, endothelial cells (ECs), pericytes, and skeletal muscle cells. While the mechanisms of degenerative diseases such as Parkinson's disease (PD), Alzheimer's disease (AD), and amyotrophic lateral sclerosis (ALS) have been extensively studied, our understanding of these disorders is still incomplete.

Animal models of neurodegenerative disease could help us understand the pathology and physiology of cell behavior in vivo. However, these animal models have several drawbacks in predicting drug efficacy in humans, both because of possible species-specific differences between humans and other animals, and because some of these animal models may not accurately reflect human disease. For instance, chemically induced PD mouse models (by 1-methyl-4-phenyl-1,2,3,6-tetrahydropyridine^[1]) and α -synuclein (α -Syn) transgenic mouse have been used to investigate the mechanisms of PD involved in degeneration of dopaminergic (DA) neurons in the substantia nigra pars compacta.^[2]

However, this is not a human model (and may be influenced by possible species-specific differences in pathology), and the chemically induced nature of this model only reflects some aspects of the human disease. In addition, the most common animal model of ALS uses a genetically engineered mouse to express a mutation of the human superoxide dismutase (SOD1) gene that catalyzes the dismutation of the superoxide radical into ordinary molecular oxygen or hydrogen peroxide. This mutation of the SOD1 gene was identified to be a significant cause of familial ALS^[3] leading to development of the SOD1 mouse model of ALS in 1994.^[4] Even this SOD1 mouse model, however, has been shown to be of limited utility for predicting human therapeutics. For instance, the therapeutic agents identified by this model have shown lower efficacy in humans compared to their response in the mouse model. This calls into question the utility of such preclinical data for identifying therapeutic agents that are worthy of subsequent study in humans. Furthermore, even though 90% of human ALS is classified as "sporadic" SOD1-mutant mouse models familial, rather than sporadic ALS, thereby limiting the value of this mouse model for most ALS patients. Adding to all these limitations, "the 3Rs" global trend (as reduction, refinement, and replacement of animal testing)^[5] signals the need to move away from animal

Dr. T. Osaki, Dr. Y. Shin, V. Sivathanu, Prof. R. D. Kamm
Department of Mechanical Engineering
Massachusetts Institutes of Technology
500 Technology Square
MIT Building, Room NE47-321, Cambridge, MA 02139, USA
E-mail: rdkamm@mit.edu

Prof. R. D. Kamm
Department of Biological Engineering
Massachusetts Institutes of Technology
500 Technology Square, MIT Building, Room NE47-321, Cambridge
MA 02139, USA

M. Campisi
Department of Mechanical and Aerospace Engineering
Politecnico di Torino
Corso Duca degli Abruzzi 24, 10129 Torino, Italy

DOI: 10.1002/adhm.201700489

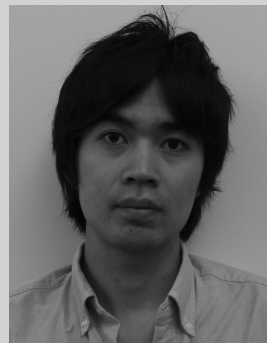
testing as much as possible in the future potentially through alternative approaches of investigating the pathology of neurodegenerative diseases *in vitro*.

Previously, 2D culture of neuronal cells has been used to test neuro-cytotoxicity. However, the drugs discovered based on 2D experiments have proven to be ineffective as potential therapies.^[6,7] Some of the 2D culture experiments used dissociated mesencephalic neurons from fetal rats,^[8] DA-neuron-derived cell lines,^[9] and embryonic stem (ES)-cell-derived dopaminergic neurons.^[10] These methods recapitulate some aspects of the physiology of PD and have been used for detailed mechanistic studies of dopaminergic neuronal degeneration in order to screen for new pharmacological agents. The DA neurotoxin 1-methyl-4-phenylpyridinium caused dopaminergic neuronal death in a system of cultured rat mesencephalic neurons. This was blocked by preincubation and simultaneous co-administration of the estrogen 17- β -estradiol. In this case, an *in vitro* model of PD was used to study the antiapoptotic effect of estrogens, and predicted that the estrogen receptor β in the midbrain might play an important role in the regulation of dopaminergic neuronal apoptosis.^[11] Thus, despite limitations of 2D culture experiments, they have demonstrated some predictive power and have proven valuable in certain cases.

3D *in vitro* cell culture systems have attracted attention for decades because they overcome some of the limitations of 2D cultures. Traditionally, these 3D cultures include cells cultured in a hydrogel, either in well plates or on Transwell membranes. These models recapitulate certain aspects of the spatial complexity of the CNS and PNS through a co-culture system containing neuronal lineage cells, endothelial lineage cells, and muscle cells. 3D cell cultures largely rely on cells growing in extracellular matrix (ECM) hydrogels including collagen, fibrin, and Matrigel. In a hydrogel, the cells self-assemble into physiological-like microstructures. For instance, neuronal cells have a 3D neurite elongation in these systems, and endothelial cells exhibit angiogenesis and vasculogenesis. Such self-assembling behavior of cells in 3D results in reconstitution of 3D biomimetic microenvironments.

In spite of these considerable advantages over 2D cultures, even these traditional 3D *in vitro* models suffer from limitations. They do not sufficiently mimic either animal models or human physiology because it is important to not only co-culture various cell types but also to (1) physically compartmentalize neuronal networks and vascular networks, (2) consider ECM composition, (3) consider biochemical effects appropriate to specific cell culture systems, and (4) apply dynamic mechanical stresses, such as fluidic stresses arising from pressure gradients as well as physical strains due to muscular contraction, in order to mimic a highly organized microenvironment such as human brain and spinal cord.^[12] Moreover, some of these traditional 3D models are neither cost effective, nor high throughput, and the protocols are often not reproducible.^[13] All these limitations need to be overcome for widespread adoption of these 3D models.

Organ-on-a-chip systems could potentially overcome most of these drawbacks of more traditional 3D methods. In this review, we discuss the state-of-the-art of microfluidic systems for modeling neurodegenerative diseases and how they mimic human physiology and pathology using various clinical studies



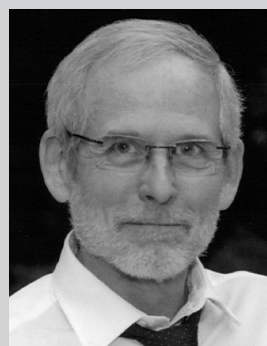
Tatsuya Osaki received his Ph.D. in Graduate school of Pure and Applied Sciences from University of Tsukuba, Japan in 2016. He joined the Bio Microsystem and Tissue Engineering Laboratory at the Yokohama National University to further his Ph.D. studies, focusing on engineering vascularized liver tissue using iPS-derived hepatocyte.

Currently, he is a postdoctoral fellow in the mechanobiology laboratory of Prof. R. D. Kamm at the Massachusetts Institute of Technology and is a member of EBICS. His research interests include neuromuscular junctions, neurovascular units in the CNS and PNS, and microfluidic devices as well as their applications to treat ALS.



Yoojin Shin received the Ph.D. degrees in mechanical engineering from Korea University, Korea in 2015 and joined the mechanobiology laboratory (R. D. Kamm) in Mechanical Engineering at MIT as a postdoctoral fellow from November 2016. Her research interests include developing microfluidic-based model of metastatic cancer,

stem cell niche, and blood-brain barrier (BBB). Her current research project is to develop a 3D Alzheimer's disease (AD)-BBB model to investigate the role of blood-brain barrier function in Alzheimer's disease pathogenesis by using a 3D microfluidic platform.



Roger Kamm is the Cecil and Ida Green Distinguished Professor of Mechanical and Biological Engineering at MIT. A primary objective of Kamm's research is the application of fundamentals in mechanics to better understand essential biological and physiological phenomena. Recently, his attention has focused on cellular force sensation, cell population dynamics, and the development of new microfluidic platforms for studies of angiogenesis and metastatic cancer.

including screening of new drugs and understanding of disease mechanism. First, we describe the advantages of microfluidic systems in modeling neurodegenerative diseases. Second, we present recent studies of brain-on-a-chip microfluidic culture

platforms that represent physiology and pathology focusing on AD, PD, and Huntington's disease (HD) as well as spinal-cord-on-a-chip methods focusing on ALS. Finally, we close with the current limitations of these strategies and speculate on potential future strategies to overcome them.

2. Microfluidic Cell Culture Systems

2.1. Microfluidic Systems in the Study of Cell Biology

Previous models used to study fundamental aspects of cell biology typically involved cell culture in culture dishes (2D) or hydrogels (3D) in which the cellular response to various external biochemical or biophysical stimuli was observed. Due to the simplicity of these systems, however, it is often difficult to understand the 3D complex structure and function of human organs, and to mimic the complex mechanical and biochemical microenvironment, which is known to strongly influence the cell function in the human body. In the late 20th century, with the advent of microfabrication techniques integrated into microfluidic systems, the limitations of traditional cell culture models were overcome, and techniques were developed to emulate the characteristic structure of tissues or organs of human or animals beyond simple cell culture.^[14] Microfluidic systems for cell culture are generally fabricated using microfabrication methods such as photolithography. A photoresist (PR) such as SU-8 is uniformly coated on the silicon wafer, and UV light is applied to the PR through the transparency photomask, with desired micropatterns. The micropatterns remain on the PR by developing and etching away the exposed part (as a positive PR) or the nonexposed part (as a negative PR). These standard soft lithography methods are widely used for the microfluidic systems in biotechnology applications.^[15] For example, polydimethylsiloxane (PDMS) has been generally used as a soft lithography material with the advantages including good biocompatibility, transparency, gas permeability, and optical transparency.^[16] It is also an electrically and thermally insulating material so that electrical circuits can be applied within the system as further described in Section 2.7.

Microfluidics-based cell culture systems, which have been used for simulating physiological and pathological phenomena or emulating *in vivo* structure from cell to organ level, generally consist of single microchambers^[17] or multiple microchambers with microchannel or microgroove arrays connecting each microchamber.^[18] In the initial stages of microfluidic system development, cell biology studies were mainly limited to 2D culture. One of the applications has been to create chemical gradients within a microchamber or across the microchannel or microgroove arrays by exploiting laminar flow (low Reynolds number), in order to provide graded stimuli to the contained cells.^[19] Biological processes such as cell differentiation,^[20,21] neurite extension of neuronal cells,^[22,23] and cell migration (e.g., neutrophil chemotaxis^[24] and cancer cell migration^[25]), which are affected by chemical concentration gradients, have been widely studied using the 2D microfluidic system. However, the 2D system has many limitations, most importantly that it fails to mimic the 3D microenvironment and other physiological features of the human tissue or organ unit.

To overcome these shortcomings, a 3D microfluidic system incorporating a biocompatible hydrogel scaffold, which can provide 3D microenvironment to cells with well-defined biochemical and biophysical stimuli, has been developed.^[26,27] In a 3D microfluidic system, various hydrogels or ECM materials (e.g., collagen, fibrin, and Matrigel) can be injected into the micropatterned structures, driven by surface tension, to mimic the ECM. Cells can be seeded either on hydrogel or patterned inside a hydrogel in various configurations such as single cells or as spheroids, and cultured in 3D with or without chemical gradients generated within the hydrogel. This system can also allow the study of 3D cell–cell interactions in hydrogels or ECM by enabling co-culture of multiple cell types.^[27] For example, 3D interaction between various cells such as cancer cells and endothelial cells,^[28] stem cells and various stromal cells,^[29,30] and hepatocyte and endothelial cells^[31] have been studied in 3D microfluidic systems. In addition, multilayered microfluidic systems have been developed by sandwiching a porous membrane between two microchannels. In such systems, one can apply different conditions to each layer and mechanical strain cells by stretching the membrane using an integral vacuum system (e.g., lung-on-a-chip).^[32] Recently, microfluidic systems have also enabled hydrogel-free 3D cell culture of spheroids or organoids. Integration of microwells or hanging drop techniques into a microfluidic system enables new insights into study of tissues or organ level interactions and facilitates various applications including cytotoxicity and drug tests.^[33]

2.2. Microfluidic Systems for Modeling Neurodegenerative Diseases

3D microfluidic cell culture systems provide significant advantages compared to typical 2D cell cultures in flasks, dishes, and well plates. First, microfluidic devices, often fabricated using PDMS, as described above, are highly customizable to meet the specific requirements for each cellular system and each experiment. For example, in order to model the human lung, Huh et al. showed that multilayered PDMS channels containing different cell types could be used to mimic organ level lung function.^[32] In this work, vacuum-assisted stretch of a thin flexible membrane on which the epithelial and endothelial cells grow could simulate the active physical microenvironment of breathing. In addition, micropillar structures could be fabricated in these chambers to encapsulate and compartmentalize the target cells^[34,35] either as a collection of sparsely distributed single cells or as a dense cluster of cells, also called a spheroid.^[36] Overall, microfluidic systems such as this lung-on-a-chip system, which are highly customizable in terms of structure, with specific cell–cell interactions and specific biochemical and mechanical microenvironment, could allow for complex yet specialized organ-specific *in vitro* models.

Second, microfluidic systems allow cell cultures with far fewer cells and a much smaller quantity of cell culture medium compared to traditional cell culture systems. This is a considerable advantage because in many cases obtaining a pure differentiated cell population in sufficient quantity is quite time-consuming and expensive. For instance, it takes about a month to differentiate induced pluripotent stem (iPS)-derived^[37] and ES-derived

cells, to obtain well-differentiated mature cells such as neurons. This is expensive due to the limited differentiation efficiency of current protocols. Hence, microfluidic devices that use fewer cells save time and are less expensive compared to typical 2D cell culture platforms. Furthermore, microfluidic cell culture offers reduced consumption of reagents, reduced contamination risk, and efficient high-throughput experimentation. It allows us to reduce the cell population to a few hundreds of cells, or even a single cell,^[38] making it possible to capture perturbations to individual cells. We could also reduce the use of expensive growth factors such as basic fibroblast growth factor (FGF) and activin that are necessary to differentiate and maintain iPS-derived mature cells. Finally, it also allows us to increase the spatial and temporal resolution for a given experimental setup.

Other advantages of microfluidic cell culture include the ability to incorporate analytical biosensors into the culture platform, to detect physiological parameters, to analyze external stimuli in situ, and to noninvasively probe cellular behavior.^[39] These biosensors could provide rapid and sensitive measurements using a small number of cells and low reagent volumes. Finally, microfluidic devices have the ability to perform perfusion culture to apply flow and shear stresses that may be necessary to mimic physiological conditions. Although external equipment such as syringe pumps or peristaltic pumps and tubing may be necessary, the connection between the tube and device is relatively straightforward. In addition, in many cases, flow can be generated by a simple hydrostatic head. Overall, there are a variety of microfluidic cell culture devices, each having distinct benefits offering great versatility. Undoubtedly, these microfluidic cell culture systems will continue to improve in the future, further adding to their advantages over traditional 2D cell culture systems.

2.3. The Role of Cell–Cell Interactions

2.3.1. The Main Cell Types in the CNS and PNS

The CNS and PNS are complex networks consisting of mixtures of neuronal and glial cells in CNS or ganglia in PNS with

other surrounding cells. The brain, for example, is the most complex organ in human body containing numerous cell types including neurons, glial cells, neural stem cells (NSCs), and brain vascular endothelial lineage cells (**Figure 1**).

Neurons are one of the major cell types in the CNS and the PNS, which electrically and chemically transmit information via synapses with other neurons, astrocytes, and interneurons. There are an estimated 100 billion neurons in the human brain, forming neuronal networks by interacting with glial cells.^[40] A typical neuron consists of a cell body with dendrites giving rise to a complex “dendritic tree” and an axon that is a specialized long cellular extension. Neurons communicate by chemical and electrical synapses in a process known as neurotransmission. The release of neurotransmitters triggers an action potential and propagating electrical signal. It is generated by exploiting the electrically excitable membrane of the neuron.

Glial cells are the most abundant cell type in the brain, which are 2–10 times more prevalent than neurons in the vertebrate central nervous system. Glial cells, including oligodendrocytes, astrocytes, and microglia,^[41] contribute to neuronal function and connectivity through cell–cell signaling and influence neurotransmission through nutrient and oxygen support.^[42]

Oligodendrocytes support the formation of a myelin sheath that wraps around axons and augments their function. The myelin sheath plays a central role in helping to increase the propagation speed of impulses along a myelinated fiber, resulting in stabilization of electrical signal transmission. In addition to physical support, they also chemically influence survival and function of neurons by releasing growth factors such as Brain-derived neurotrophic factor (BDNF), Neurotrophin-3 (NT-3) and Nerve growth factor (NGF).^[43]

Astrocytes play a multifunctional role in supporting neuronal synapses and blood vessels in the brain. They act as “passive support cells” for electrically active neurons and are primarily responsible for cellular homeostasis of the CNS. Other representative functions of astrocytes are to support and maintain the blood–brain barrier (BBB) through physical and chemical interactions with endothelial cells and pericytes. They cover endothelial cells with endfeet and secrete various cytokines

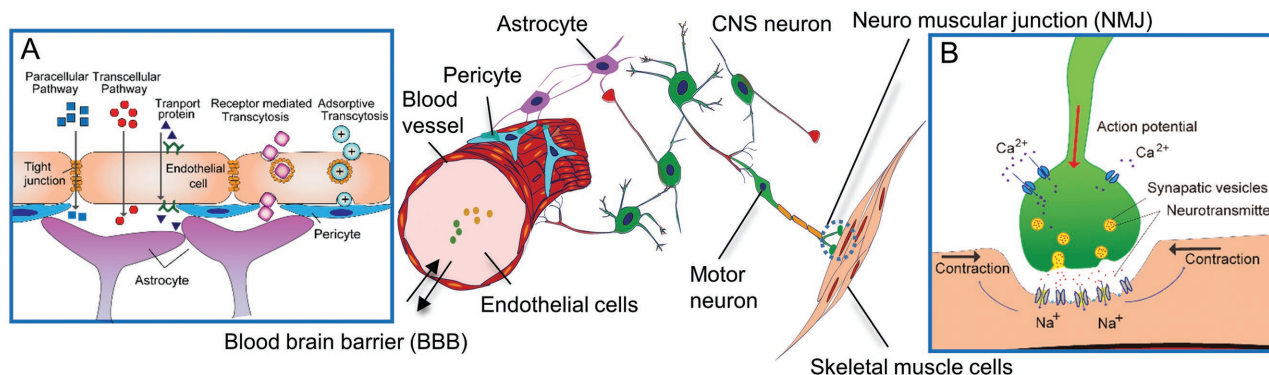


Figure 1. The main players in neurodegenerative disease. In the CNS and PNS, CNS neurons, peripheral motor neurons, astrocytes, endothelial cells, pericytes and skeletal myoblasts interact with each other and with complex cell–cell junctions and various types of ECM (e.g., lecticans, glycoproteins, proteoglycans, hyaluronic acid, collagen and laminin). In particular, the blood–brain barrier (BBB) in brain and neuromuscular junctions of the motor unit play an important role in the pathogenesis of various neurodegenerative diseases. A) BBB is a brain specific barrier, which has a very low permeability and specific transporters for communication between the inside and outside of the brain vasculature. B) The neuromuscular junction is a chemical synapse formed by the contact between motor neurons and muscle fibers. Motor neurons transmit signals to the muscle by releasing acetylcholine (ACh), causing muscle contraction.

including Glial cell line-derived neurotrophic factor (GDNF), angiopoietin-1 (ANG-1), and Sonic hedgehog (SHH), which maintain and support BBB tight junction integrity.^[44]

Microglia are the brain's resident immune cells, which are important regulators of neuroimmunity against pathological insults occurred by neurodegenerative diseases, injury, and ischemia in the CNS.^[45] In an inflammatory state, microglia are activated to survey the CNS and are capable of secreting high levels of cytokines such as interleukin-1 β (IL-1 β), IL-6, Tumor necrosis factor-alpha (TNF- α), CCL2 in the pro-inflammatory state and IL-10, IL-4, and transforming growth factor beta (TGF- β), in the anti-inflammatory state.^[46] In addition, recent studies have found that microglia are closely associated with amyloid beta (A β) deposition in AD, but their AD-related inflammatory functions still remain to be elucidated.^[47]

Brain endothelial cells (bECs), the primary component of the BBB, are an important component of the brain. The BBB differs from the endothelial barrier of other organs in several key ways; there are specific tight junction proteins that minimize paracellular transport leading to a BBB with low permeability, and there are specific transporters expressed that selectively control the transport of molecules (Figure 1Ai).^[48,49]

Pericytes are also an important component of the BBB in combination with brain endothelial cells and astrocytes. Pericytes interact with the brain endothelium to regulate BBB integrity and function by having direct contact with the capillary wall via N-cadherins (adherent junction protein), CX43 (gap junction protein), cross-talk between platelet-derived growth factor β (PDGF- β) and its receptor (PDGFR- β), TGF β /TGF β R2, and notch signaling. Pericytes play an important role not only in the maintenance of BBB integrity but also in the regulation of blood flow.^[50,51] Recently, researchers have shown that pericyte degradation leads to BBB breakdown, which is found in several neurodegenerative diseases. For instance, in AD, A β has the effect of degrading pericytes, leading to an impaired BBB. Because of these findings, the importance of pericytes has been raised in the study of neurodegenerative diseases.^[50]

2.3.2. Cell–Cell Interactions in the CNS

Most neuropathology studies use these neurons due to their central role in brain function. However, in recent years, there has been an increasing perception that integrated brain function and dysfunction occur due to the complex interactions of networks of multiple cell types.^[52] Brain is composed of multiple units including neuron–glia and neurovascular units which are maintained by physical and chemical interactions among groups of cells.^[53] Since most neurodegenerative diseases are caused by at least one type of dysfunction in cell–cell communication, elucidating the mechanisms of cell–cell interactions and their role in brain homeostasis and dysfunction is essential to understand the pathogenesis of neurodegenerative diseases.^[54,55] Neuron–glia interactions are fundamental for regulating the critical functions in brain health and disease with roles in information processing, axonal conduction, and neurotransmission.^[55,56] Also, the neurovascular unit, which

is the functional unit of the BBB, is composed of the cerebral microvascular endothelium together with pericytes, the endfeet of astrocytes, adjacent neurons, and basal lamina.^[57] An increasing body of evidence suggests that alterations in neuron–glial interactions and dysfunction of the neurovascular unit are associated with neurodegenerative diseases including Alzheimer's disease and Parkinson's disease.^[58] For instance, recently, researchers have identified leakage in the BBB in early AD patients with the decreased expression of tight junction proteins and disruption of the BBB clearance system which seems to increase the risk of AD.^[59] This will be discussed in further detail in sections 3.1.3 and 3.1.4.

2.3.3. Cell–Cell Interactions in the PNS

The PNS is divided into the autonomic, sensory, and somatic nervous systems. The autonomic nervous system controls involuntary muscles such as smooth and cardiac muscle^[60] while the sensory nervous system, which consists of sensory neurons, is responsible for processing sensory information. The specific receptors (e.g., chemoreceptors, photoreceptors, mechanoreceptors, and thermoreceptors) to a stimulus transduce the signal into an electrical action potential via the sensory nervous system. The somatic nervous system regulates skeletal muscle to control body movement, stimulating muscle contraction, as well as external sensory organs such as the skin and consists of lower motor neurons and upper motor neurons. In particular, dysfunction of motor neurons is crucial to the incidence of motor neuron diseases that are a form of neurological disorders. Such motor neuron diseases include ALS, primary lateral sclerosis, progressive muscular atrophy, progressive bulbar palsy, pseudobulbar palsy, and spinal muscular atrophies.^[61]

Motor neurons regulate the transport of electrical signals to muscle, triggering it to either contract or relax. Its basic structure includes a receptor on one end and a transmitter on the other end connected by an elongated axon. A motor neuron forms a motor unit with skeletal muscle fibers innervated by axonal terminals of just a single α motor neuron.^[62] An action potential generated by a motor neuron normally brings all muscle fibers to threshold via neuromuscular junctions (NMJs) (Figure 1B). An NMJ consists of a neuron and a skeletal muscle cell. There are two membranes: the pre- and post-synaptic membranes, with a distinct space between the two called the synaptic cleft.^[63] Small spherical vesicles are present, which contain neurotransmitters that shuttle between membranes. Calcium enters the excited motor neuron, which in turn causes exocytosis of the neurotransmitter. Acetylcholine (ACh) is the neurotransmitter secreted by the somatic motor neurons. Dysfunction of the neuromuscular junction causes some disorders such as myasthenia gravis,^[64] botulinum toxin,^[65] and Eaton–Lambert syndrome.^[66] The neuromuscular junction can also malfunction when exposed to certain antibiotics, organophosphates (a type of insecticide), curare (a toxin derived from plants), and gases used in chemical warfare. Some of these chemicals act on the NMJ by preventing the breakdown of acetylcholine after the transmission of the nerve impulse.

2.3.4. Limitations of Current Systems in Studying Cell–Cell Interactions

Despite numerous efforts dedicated to studying cell–cell interactions using *in vivo* and *in vitro* systems, the mechanisms of the cell–cell interactions in CNS and PNS are still unclear, mostly due to the inherent complexity of cell–cell interactions in these systems. For instance, although *in vivo* studies have the advantage of emulating physiological complexity and maintaining the whole organism intact, it is difficult to accurately decouple the specific cell–cell interactions of interest from interference of other cells and tissues. On the other hand, *in vitro* systems trade off the high complexity of *in vivo* systems with more precise control of fewer parameters, letting researchers conduct more controlled studies.^[67] However, current *in vitro* systems tend to be too simple to represent the complex nature of *in vivo* physiology.

2.3.5. Microfluidic Systems to Study Cell–Cell Interactions

Microfluidic technology has emerged as a powerful tool for studying such multicellular phenomena with a balance of complexity and control. It allows reconstitution of a complex physiological microenvironment with enhanced control compared to *in vivo* systems. It also enables precise spatiotemporal control of the 3D cellular and noncellular microenvironment, integration of multiple functional assays in a single experimental platform, enhanced imaging capabilities, and a reduction in reagent volume as well as tissue sample size.^[27] Recently, many microfluidic co-culture systems have also been developed to monitor cell–cell interactions via paracrine signaling (soluble molecules) or juxtacrine signaling (direct physical contact) between different cell types in a more precisely controlled manner.^[68]

Compartmentalized microfluidic systems enable superior spatiotemporal control over each of the tunable environmental parameters of cell culture. For instance, Taylor et al. developed a microfluidic system composed of two compartments connected by microchannel arrays (**Figures 2H, 4B,C, and 5A**).^[23] This system has widely been used for neuron–glia interactions by separating axons from soma and allowing axons to interact with glia cells.^[69] Huh et al. reported a compartmentalized microfluidic system with a porous membrane separating two parallel, upper and lower, microchannels.^[32] This system could be used for studies of cell–cell interaction by enabling paracrine signaling interaction through the pores.^[12,70] Such systems could also incorporate monolithic microfabricated valves in order to control flow direction by actuating valves.^[71] This co-culture system has the advantage of facilitating both spatiotemporal control of paracrine signaling and the study of unidirectional paracrine/juxtacrine signaling between cells. In addition, this microfluidic system has been modified to incorporate a 3D hydrogel scaffold through which microchannels are compartmentalized (see Hall and Sanes^[63] for the device design). This could be applied to interactions of different cell types with a more physiologically relevant 3D cellular microenvironment. Overall, this system is advantageous in its flexibility to be used for a wide variety of different co-cultures, allowing both paracrine and juxtacrine signaling.^[27,72]

2.4. The Role of ECM in Modeling Neurodegenerative Diseases

Traditionally used 2D neuronal culture systems are limited in their ability to mimic the 3D microenvironment of *in vivo* systems. Even though ECM coatings are used in these 2D systems, they do not sufficiently have the physiological ECM's 3D architecture. The ECM scaffold is one of the most important considerations in modeling neurodegenerative diseases. The ECM composition is highly tissue specific, and incorporating an appropriate ECM is important in developing an organ-specific *in vitro* model. For instance, for *in vitro* models of neurodegenerative diseases, controlling the ECM in the various tissues involved is important in order to realistically mimic the 3D brain microenvironment. This, in turn, controls and promotes physiologically relevant cellular behaviors and activities such as cell differentiation, migration, and cell–cell interaction.

Microfluidic technologies have been widely used for 3D cell culture by incorporating ECM scaffolds, which provide micro-scale cellular niches for physiologically relevant reconstitution of 3D multicellular co-cultures. More specifically, compartmentalized microfluidic systems (CMSs) have the ability to incorporate different ECM materials for the culture of different cell types in 3D, all within the same system. This ability to spatially pattern the ECM material in a microfluidic system is a key advantage. For example, Huang et al. developed multiple discrete constructs of 3D cell-laden hydrogels to be patterned in a microfluidic device.^[84] Matrigel and collagen gel were patterned in adjacent microfluidic channels for the breast cancer cells and tumor-derived macrophages, respectively, in order to investigate cell–cell and cell–ECM interactions.

2.4.1. The Central Nervous System ECM

The structure and composition of ECM significantly influence its function in the CNS. The ECM accounts for a significant proportion of the CNS, contributes to structural stabilization of cellular networks, and acts as a source of biochemical signals for cellular function and activity. The ECM of the CNS is a large component of brain and spinal cord tissue, consisting of a dense substrata that occupies the space between neurons and glia, estimated to comprise 10–20% of the total brain volume.^[85] The ECM of adult brain has a unique composition consisting of primarily dense networks of lecticans, glycoproteins, proteoglycans, and an abundance of hyaluronic acid (HA) and tenascin family proteins.^[86] Matrix proteins that are common in many other tissues (e.g., cartilage and bone) such as fibrillary collagens and fibronectin are nearly absent in the brain. The ECM not only contributes to cellular organization and structure with biochemical and mechanical signals but also plays an important role in brain development and adult neural function. In addition, ECM is a key factor in the study of neurodegenerative diseases because ECM alterations are found to be associated with neuropathological conditions and the pathological process of neurodegenerative diseases.^[87] For example, matrix metalloproteases (MMPs) in cases of chronic neurodegeneration clearly regulate the progress of symptoms in AD and PD.^[88] Furthermore, MMPs have a key function in tissue repair processes such as angiogenesis and neurogenesis. Recently, ECM

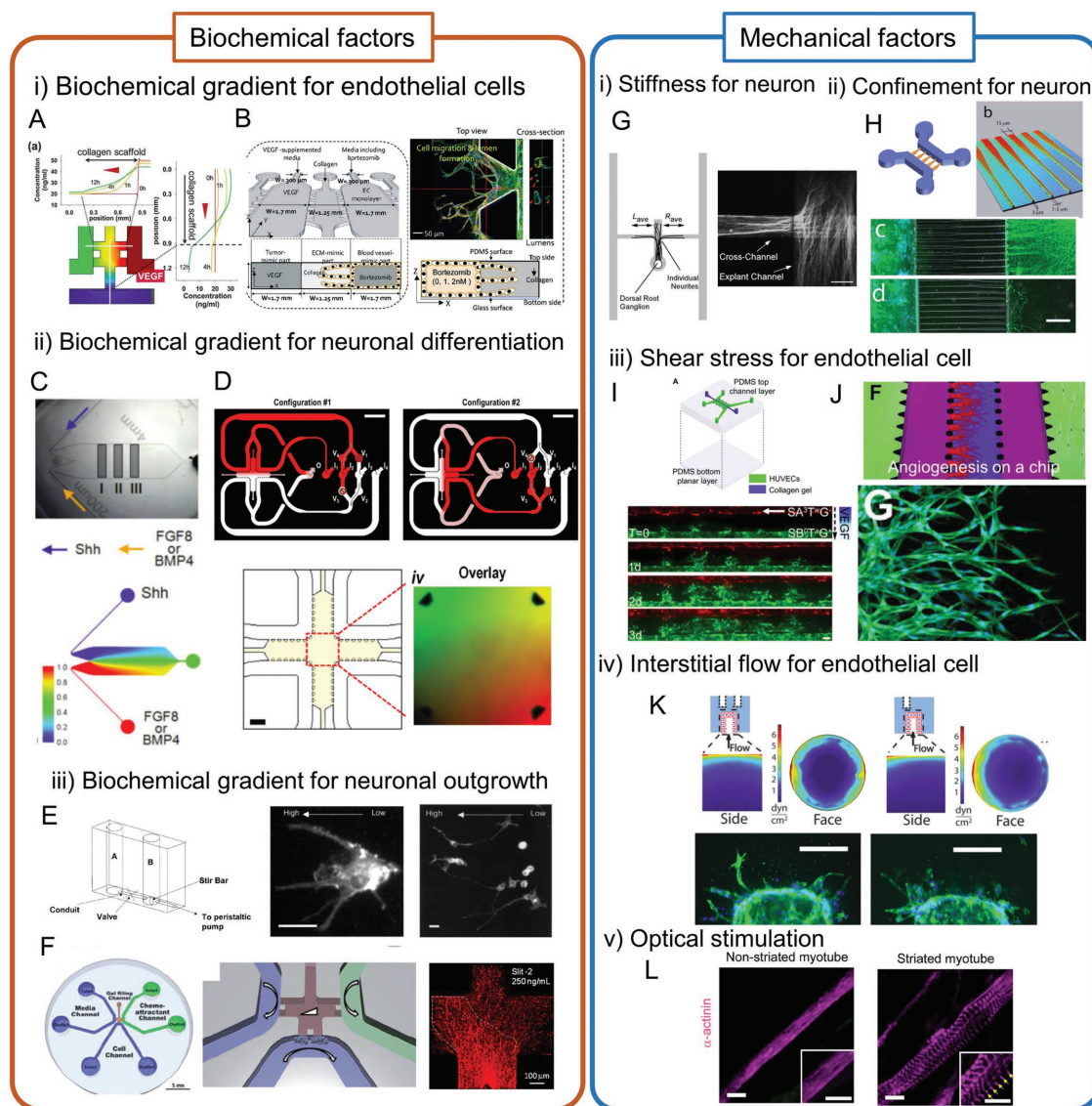


Figure 2. Biochemical and mechanical factors for neurodegenerative disease in a microfluidic device. A) A gradient of biochemical factors (VEGF and ANG-1) affects the directionality of endothelial sprouting in two orthogonal directions. Reproduced with permission.^[73] 2011, Royal Society of Chemistry. B) High-throughput screening model for an angiogenesis assay with a multichannel device to test antiangiogenesis drugs for cancer metastasis. Schematic view of the quantitative microfluidic angiogenesis screen and anticancer effect of bortezomib. Reproduced with permission.^[74] 2015, Royal Society of Chemistry. C) A microdevice generating gradients of biochemical factors (SHH, FGF8, and BMP4) related to neuronal development and differentiation of stem cells. These chemical gradients regulate the differentiation into motor neuron cells. Reproduced with permission.^[21] D) Multi-dimensional chemical gradients were generated in the cross-shaped device. A diffusion-driven linear gradient was generated within its central collagen gel region and orthogonal to it (90° rotation), a second gradient was generated (red and green fluorescent tracers). Reproduced with permission.^[75] E) Simple immobilized NGF gradient device used for investigation of neuronal outgrowth of PC12 cells. The dendrites of PC12 elongated toward the higher concentration side of the NGF gradient. Reproduced with permission.^[76] F) Directionality of neuronal outgrowth in a hydrogel was observed in a microdevice with a biochemical gradient of netrin-1, brain pulp, or slit2. Reproduced with permission.^[77] 2011, Royal Society of Chemistry. Mechanical factors also affect the behavior of neurons, endothelial cells, and skeletal myoblasts. G) Stiffness of the scaffold has a significant effect on migration and proliferation of neurons. An H-shaped gel device was used to investigate the relationship between mechanical stiffness and cell behavior. Reproduced with permission.^[78] H) Axonal guidance was controlled by the confinement of channels in a microfluidic device. Many axons extend from the wide side to the narrow side, although only a few grow in the opposite direction. Reproduced with permission.^[79] 2011, Royal Society of Chemistry. I) Shear stress attenuates VEGF-driven angiogenic sprouting by decreasing of EC proliferation and migration. Reproduced with permission.^[80] 2011, National Academy of Sciences. J) Multichannel microfluidic device was used to decouple chemical factors from mechanical factors. Interstitial flow induced cytoskeletal reorganization of ECs comprising microvascular networks. Reproduced with permission.^[81] 2013, Royal Society of Chemistry. K) Interstitial flow across endothelialized vascular wall induces angiogenic sprouting. Microfluidic device with endothelialized void channel and nozzle-shaped channel could be used to investigate the relationship between interstitial flow and sprouting and migration of EC. Reproduced with permission.^[82] 2014, National Academy of Sciences. L) Optical stimulation of skeletal myoblast which is genetically engineered to express ChR2 improves the differentiation of myoblasts into mature myotubes. Adequate training (1 Hz) helps the formation of sarcomeric structure of myotubes. Reproduced with permission.^[83] 2015, Nature Publishing Group.

scaffolds for emulating the brain ECM have been developed with numerous natural^[89] or synthetic materials^[90] with a wide range of physical and chemical properties.

Natural polymers such as HA, lecticans, glycoproteins, and proteoglycans have been used as ECM scaffolds to mimic neural environment due to their biocompatibility and the structural resemblance of ECM in the tissue of origin.^[91] Additionally, ECM materials including collagen, Matrigel, gelatin, and fibrin are used for in vitro vascular^[92] and neuronal network formation^[93] in the context of brain models, particularly in the context of glioblastoma, even though these materials are not common in healthy brain tissue.^[94] Also, they have the advantage of retaining growth factors and adhesion molecules that promote cell attachment, growth, or differentiation. However, there are still limitations in mimicking brain-specific ECM. To overcome these limitations, techniques that incorporate natural polymers or functional molecules with synthetic polymer templates have been developed to better mimic brain compatible ECM.^[95,96] A technique to extract ECM from brain tissues has been developed to provide a natural brain ECM for neural cells. The natural ECM scaffold decellularized from tissues has the advantage of retaining structures such as the ECM fibers as well as proteins of the native ECM, both of which modulate behaviors of neural cells and support neuronal network formation. Several groups have developed and introduced decellularization protocols to extract ECM from porcine, rat, and fetal brains with physical, chemical, and enzymatic methods.^[97,98] Differentiation, neuronal network formation, and neural cellular behavior are all promoted when the decellularized brain ECM is used.^[97]

Additionally, there are many synthetic polymers that could be introduced as a suitable scaffold for supporting neural cell growth and functions. They could be used for various applications taking advantage of the flexibility to control a variety of physical parameters such as pore size, fiber scale, and stiffness, and chemical parameters like pH and surface modification with cellular molecules. These synthetic polymers include poly(ethylene glycol),^[99] poly L-lactic acid,^[100] poly D, and L-lactic-co-glycolic acid^[96] polymer hydrogels.

2.4.2. The Peripheral Nervous System ECM

In contrast to ECM in the CNS, laminin and collagen play an essential role in PNS development.^[101] Laminin signals regulate Schwann cell proliferation, survival, and cytoskeletal dynamics, which helps the formation of the myelin sheath around neurons. During PNS development, laminin also coordinates Schwann cell elongation at later stages of myelination through interaction with the DG-DRP2-periaxin complex.^[102,103] Collagen and its receptor also promote Schwann cell adhesion and myelination as well as neurite elongation through regulation of intracellular signaling in vivo. Even in the case of in vitro culture of neuronal cells, many researchers showed that laminin also helps the differentiation of neural stem cells into motor neurons. Also, different subtypes of laminin have been shown to have advantages for different cells. For instance, laminin 511, rather than 211 and 411, has better adhesive properties for human iPS cells.^[104] In particular, E8 fragments of laminin

511 support the long-term self-renewal and adhesion of human Embryonic stem cell (ESC) and human iPS cells compared to Matrigel, which is made up of various subtypes of laminins.^[105] The heparin-binding domain of laminin is responsible for its effects on neuronal outgrowth and survival.^[106] Other groups showed that the interaction between laminin-2 expressed by oligodendrocytes and laminin-binding integrins may play an important role in the signaling that stimulates oligodendrocytes to support the formation of the myelin membrane required for the myelin sheath.^[107] In the case of skeletal myoblasts, Matrigel significantly improves their differentiation. Grefte et al. showed that muscle progenitor cells, both in 2D and 3D, lose their differentiation capacity in collagen but not in Matrigel^[108] (one caveat to this is that Matrigel does contain growth factors). In addition to the above, Matrigel supports survival and neuronal differentiation of ES-derived neural stem cells.^[109]

2.5. Influence of Biochemical Factors

Soluble factors such as cytokines and chemokines play an important role in the CNS because neural networks and other brain compartments such as the neurovascular unit have continuous paracrine interactions. These factors regulate not only neurodevelopment and inflammation but also synaptic transmission.^[110] Soluble factors are locally transported to cells by many different flow conditions including interstitial fluid with a local concentration gradient within the interstitium. The cytokines and chemokines have a crucial role in immune functions in the nervous system under physiological and pathological conditions. Especially in pathological states such as infection and other diseases during which microglial cells are activated, these cells release inflammatory factors that mediate neural cell damage and lead to transendothelial migration of immune cells across the BBB. For example, IL-6 is known as a neurodegenerative disease-related cytokine. In the pathogenesis of AD, microgliosis, a reactive microglia in a pathogenic state, is induced by A β . These reactive microglia have increased IL-6 production, which is an abnormal immune reaction to A β in the brain, that results in enhanced neuronal damage by A β . Increased expression of many cytokines including IL-1, IL-2, IL-4, IL-6, and TNF- α is also associated with pathogenesis in Parkinson's disease.^[111]

Gradients of several biochemical factors, some of which were mentioned earlier, are important in development of the CNS and PNS. Microfluidic systems have enabled us to create biochemical factor gradients using spatially defined flow patterns. This helps enable studies of cellular behavior and generate physiologically or pathologically relevant fluid condition such as maintaining constant soluble microenvironment with a large surface area-to-volume ratio. Furthermore, the ease of creating chemical gradients in microfluidic systems allows the researchers to test the dose response of several chemicals in high throughput in the same system. Many groups have generated a stable gradient of soluble biochemical factors of various kinds. For instance, a concentration gradient of growth factors and chemoattractants was generated and maintained under dynamic conditions with continuous flow (using a syringe pump) in a microfluidic channel to investigate the concentration dependence of neural stem cell growth and differentiation or neural cell responses.^[75] Microfluidic systems have also been

used to create growth factor gradients under static conditions with standard tools (e.g., pipettes) in the absence of continuous syringe pump driven flow, with the gradient generated by differences in concentration across a channel. Such methods have been used by many groups due to their ease of use.

2.5.1. Biochemical Gradients for Endothelial Cells

Angiogenesis and vasculogenesis are important biological processes even in the CNS and PNS. Gradients of several biochemical factors influence these processes and microfluidic technologies could be used to generate these gradients. The generation of multiple gradients could enable studies of synergistic effects of various soluble factors on cell behavior. For example, vascular endothelial growth factor (VEGF) is one of the most crucial growth factors for forming microvascular networks as it has a dramatic effect on migration and proliferation of endothelial cells through VEGF receptor-2 signaling. VEGF determines the directionality of angiogenic sprouting to by guiding an endothelial tip cell to high concentrations of VEGF.^[112] PDGF,^[113] ANG-1, TGF- β ,^[114] and FGF^[115] also regulate the maintenance of the vascular wall through ANG-1 and Tie-2 signaling as well as Notch and Wnt signaling.^[116] These growth factors interact synergistically with each other for the formation and stabilization of vascular networks. In a microfluidic device, it is straightforward to generate a linear profile of chemical concentrations across a contained hydrogel (such as collagen gel or fibrin gel) because the presence of porous hydrogel allows diffusion while at the same time suppressing convective flows. Therefore, various types of gradient profiles can be generated by varying the configurations and architecture of microfluidic channels. For example, a gradient profile across the gel channels can be generated by the microdevice with a single hydrogel channel between two medium channels^[117] or two hydrogel channels between three medium channels.^[118] Additionally, two linear gradients of different growth factors, such as VEGF and ANG-1, can be generated in two orthogonal directions in microfluidic devices with a hydrogel surrounded by three channels.^[73] Using these types of devices, the opposing effects of ANG-1 (stabilizing) and VEGF (proliferating) on the endothelial cells have been elucidated in *in vitro* experiments. Such a platform has aided in the investigation of interactions and potential synergistic effects of different types of growth factors, with different cell types in a range of physical and chemical microenvironments (Figure 2A,B).^[74]

2.5.2. Biochemical Gradients for Neuronal Cells

In neuronal vertebrate development, a multiplicity of signaling molecules passes between different tissues and organs. These molecules play important roles in bridging the gap between cellular differentiation and organogenesis in the process of neurulation.^[119] A specific cell is believed to recognize its position in a concentration gradient of extracellular signaling molecules such as bone morphogenetic protein 4 (BMP4), FGF, SHH, retinoic acid (RA), Wnt3 in the process of shape change of the neural plate as well as folding and patterning of the neural

tube.^[120] The cell's developmental fate is hierarchically determined by a spatially and temporally defined concentration gradient of these chemical factors. In particular, because RA and SHH concentrations regulate neural cell's fate from neural stem cells to neurons in the regions of forebrain, midbrain, hindbrain, and spinal cord,^[121] a gradient of these chemical factors has been generated in microfluidic devices in many *in vitro* studies. A gradient of SHH secreted from the notochord and cells of the floor plate provides ventral topographic information by regulating the expression of homeodomain and basic helix-loop-helix transcription factors.^[122] Therefore, controlling concentration gradients of these molecules could be used to study the regulation of differentiation of CNS neurons.

As an example of modeling neurulation in microfluidic systems using chemical gradients, Park et al. demonstrated the generation of a cytokine gradient in a simple microfluidic chip under static culture (Figure 2C). This device has two micropipettes, inlet and outlet reservoirs, and a cellulose membrane. It was used to generate orthogonal gradients of SHH and BMP4 to differentiate neural progenitor cells to neurons, generating neural networks. They also showed that the opposing effects of agonist (SHH) and antagonist (BMP4) on the proliferation and differentiation of hESC-derived neurons could be successfully recapitulated by means of concentration gradients in the microfluidic device. Demers et al. demonstrated the generation of four different molecular gradients in multilayered microfluidic devices for the reconstruction of neural tube by means of mimicking the primary aspects of the diffusion-based patterning of the neural tube.^[123] Flow channels running under the cell culture channels supply nutrients and desired guidance molecules to the cells. Morphogen concentration gradients (RA, SHH, BMP4, and FGF) are generated across the chamber using the vias (vertical channels fluidically connecting multiple layers) to control motor neuron differentiation. This gradient generating device has a significant advantage over traditional 2D cell culture systems because it allows the establishment of more biomimetic microenvironments to understand complex developmental processes and improvement of differentiation efficacy of neurons through complicated signaling pathways and transcription factor interactions. Our group also developed a microfluidic device design to generate sequential and orthogonal gradients (Figure 2D).^[75] The cross-shaped design of this microfluidic device allows the generation of a diffusion-driven linear gradient within its central collagen gel region. This gradient could be rotated by 90° to generate a sequential orthogonal gradient. The design also allows a separate gradient to be generated at 90° to the original one, thereby enabling the formation and maintenance of multidimensional gradients. These concentration gradients of RA and SHH improve the differentiation of motor neuron cells from mouse ES cells.

Chemical gradients also have effects other than those we discussed so far. For instance, they affect the orientation of neurite elongation in hydrogels. Kapur and Shoichet also showed that immobilized gradients of nerve growth factor guide neurite outgrowth of PC12 cells in microfluidic device (Figure 2E).^[76] They clearly showed that PC12 cell neurites are strongly guided and oriented by immobilized NGF concentration gradients. Kothapalli et al. demonstrated that a novel microfluidic device with three medium channels and a

single gel channel could be applied to investigate the neurite guidance by generating concentration gradients of netrin-1, brain pulp, and slit-2 (Figure 2F).^[77] These high-throughput methods of using chemical gradient in microfluidic devices should be further developed, refined, and standardized. The establishment of these techniques along with precise methods of differentiation to neurons is necessary in order to use them to understand the mechanisms of neurodegenerative diseases.

2.6. Influence of Mechanical Factors

Cell behavior in CNS and PNS is regulated not only by biochemical factors discussed above but also by mechanical factors. Understanding the role of mechanical factors and their link to biochemical factors and eventually biological function is essential for understanding and recapitulating the pathology of neurodegenerative diseases. These mechanical factors include (1) stiffness, (2) confinement, (3) shear stress, (4) interstitial flow, and (5) optically induced exercise training (for muscle). In the nervous system, mechanical signaling via mechanotransduction is also an important factor for cell or tissue behavior in neurogenesis and the pathogenesis of neurodegenerative diseases. Mechanical factors also affect cellular morphology, proliferation, phenotype, and migration.

2.6.1. Mechanical Factors that Affect Neural Cells

Many *in vitro* studies that culture cells on the substrates of defined stiffness have shown that mechanical properties determine the differentiation of neural stem cells and growth of neural cells. When brain cortical cells are cultured on soft or stiff substrates, their growth preference of each cell type depends on the stiffness. Neurons preferentially grow on soft substrates, while glial cells actively grow and proliferate on stiffer substrates.^[124] Neurite outgrowth also depends on substrate stiffness. In Sundararaghavan et al., a gradient in substrate stiffness in a microfluidic device was used to study the effect of stiffness gradients on axon outgrowth using an H-shaped gel chamber.^[78] They showed that axons of neurons grow and migrate in the direction of decreasing stiffness (Figure 2G). Geometric confinement also affects the directionality of axon outgrowth, as demonstrated when axons were allowed to grow into microgrooves of decreasing the width of thin channels. While many axons migrate from the wide side to narrow side, very few grow from narrow side to wide side (Figure 2H).^[79]

2.6.2. Mechanical Factors that Affect Endothelial Cells

To maintain homeostasis of the vascular system, endothelial cells are regulated by shear stress and interstitial flow. Hattori et al. developed a perfusable microfluidic device that provides three different levels of shear stress (0, 4.9, and 10.0 dyn cm⁻²) using a peristaltic pump for analysis of vascular endothelial (human umbilical vein endothelial cells) functions.^[125] They

clearly showed that endothelial cells attached to microchannels align in the direction of flow under conditions of shear stress above 4.9 dyn cm⁻², and that gene expression of endothelial nitric oxide synthase (eNOS) and thrombomodulin (THBD) increases in a shear stress-dependent manner. eNOS and THBD contribute to an atheroprotective effect by increasing NO production and preventing coagulation. Thus, shear stress clearly plays an important role in maintaining a healthy endothelium. Song and Munn investigated how fluidic force affects the sprouting of endothelial cells in microfluidic devices with a single gel channel.^[80] They found that physiological shear stress (0.01 and 0.3 Pa) attenuates VEGF-driven angiogenic sprouting. This attenuation by shear stress was accompanied by a decrease in EC proliferation and NO production (Figure 2I). In addition, Kim et al. established 3D perfusable microvascular networks on a chip.^[81] They also described that fluid flow induced cytoskeleton reorganization of the ECs comprising the microvascular networks which showed a distinct distribution of F-actin microfilaments compared to static conditions although dense F-actin bundles preferentially localized at the periphery of endothelial cells in the absence of fluid flow (Figure 2J). On the other hand, Galie et al. showed that luminal flow induced sprouting is triggered by a common threshold of shear stress in a microfluidic device.^[82] This threshold response occurs regardless of whether the flow is transmural or luminal. They showed that shear stress above 1 Pa threshold upregulates the expression of MMP-1. They also showed that interstitial flow across the vascular wall tends to promote angiogenic sprouting (Figure 2K). To test this, they fabricated an endothelialized microchannel with one or two cell-free channels placed opposite to the cell-seeded region and nozzle shaped microchannel.

2.6.3. Mechanical Factors that Affect Skeletal Muscle Cells

In the motor unit, skeletal muscle cells contract and relax due to transmission of action potentials from motor neurons. To prove that moderate training and exercise of skeletal muscle cells promote their survival and differentiation, Asano et al. showed that rhythmic stimulation of optogenetically modified cells facilitated sarcomere assembly to form the specific structural alignment of sarcomeric proteins, which are involved in muscle contraction (Figure 2L).^[83]

2.7. Methods to Probe Neural and Vascular Activities in Microfluidic Devices

2.7.1. Morphological Analysis by Immunostaining

The most common method to characterize the activity of neurons and endothelial cells is morphological analysis by immunofluorescent staining. For neuronal cells, an increase in the expression of immature neuronal markers (Tuj1, NeurD1, and TBR1) and mature neuron markers (microtubule associated protein 2 (MAP2), synaptophysin, and PSD95) and a decrease in neuronal stem cell marker (Nestin) show the maturation of neuronal networks. For identification and characterization

of specific neurons, vGluT1, vGluT2, and glutaminase for glutamatergic neurons; GAT1, GABA_B receptors 1 and 2, and GAD65 for GABAergic neurons; TH, DAT, and FOXA2 for dopaminergic neurons; and HB9, Islet1, ChAT, and SMI-32 for motor neurons were useful.^[126,127]

Regarding endothelial cells, to evaluate permeability of vascular structures, increased expression and localization of tight junction proteins at the boundary of cells are strong indicators of low permeability in vascular networks.^[128]

To measure the permeability of endothelial cells directly in macroscopic devices such as Transwell systems, transendothelial electrical resistance (TEER) measurement across the barrier is a standard noninvasive method for monitoring endothelial barrier integrity using electrodes.^[129] In such systems, it has been shown that changes in electrical resistance correspond to tight junction dynamics. In microfluidic systems, TEER can be measured by integrating a set of electrodes within the microfluidic system.^[130]

Furthermore, through the perfusion of fluorescently tagged dextrans (70, 40, and 10 kDa) and by studying their diffusion characteristics, permeability of the endothelial barrier can be evaluated.^[131,132] The rate at which dextran crosses the endothelial barrier (J) from the lumen side equals the rate at which it accumulates in the hydrogel, as is reflected in the following equation

$$J = A_b P \Delta C = \frac{d}{dt} \int C \, dV \quad (1)$$

Where A_b is the surface area of endothelial monolayer at the boundary of the gel and endothelial layer, P is the permeability coefficient, ΔC is the concentration change across the barrier, and the integral is taken over the volume (V) of the gel region.^[131]

In addition, staining of specific transporters (e.g., CAT1, ABCA1, PGP, MRP1, and TfR) on endothelial cells also shows the maturation of “brain” endothelial cells.^[133] To observe such vesicular-mediated transport, high contrast and resolution are necessary. Traditional confocal laser scanning microscopy^[134] and spinning disc fluorescent microscopy^[135] are ways to image these micrometer-scale cellular structures. In addition, 3D reconstruction of the images acquired by confocal laser microscopy helps us understand the cell and tissue structure. Moreover, multiphoton laser microscopy could help to image deeper into dense tissues such as those with spheroids and cell sheets.^[136]

2.7.2. Vascular Perfusability and Functionality

An important feature of microvascular networks in microfluidic systems is the existence of an open lumen within the networks, which leads to the networks being perfusable. To test this, a solution containing fluorescently tagged microbeads is typically introduced into microvascular networks.^[137] By flowing microbeads of differing diameter, one gains insight into the effective diameters of these microvascular networks. In addition, the perfusion of fluorescently tagged blood cells such as leukocytes sheds light on the functionality of the vasculature in terms of its inflammatory response.^[138] By stimulating endothelial cells

with cytokines such as TNF- α , endothelial cells can capture these immune cells via ICAM-1 expression on the endothelium. Consequently, we also observe a phenomenon referred to as “cell-rolling” before leukocytes extravasate.^[139] Finally, the introduction of casting agents into the vascular networks and subsequent degradation of the surrounding matrix could also be used to visualize the morphology of microvascular structures.^[140]

2.7.3. Neuronal Activity Patterns

Voltage imaging could be a method used to capture the electrical activity of each neuron in the neuronal circuit, including subthreshold excitatory and inhibitory events with sub-millisecond temporal precision and micrometer resolution.^[141] The electrical patterns and dynamics of dendritic trees with synaptic inputs and their subsequent responses could similarly be visualized. In addition, high-resolution voltage imaging could be crucial to understand dendritic integration, the electrical function of dendritic spines. Furthermore, multielectrode arrays (MEAs) have excellent temporal resolution and extended coverage, and their noninvasive manner makes them particularly suited for long-term experiments. Combining MEAs with microfluidic systems could, in principle, improve the detection of neural activity, although limited to 2D cultures. Also, practical constraints may limit their usefulness, in that it requires precise alignment for electrode–microfluidic device integration. Despite these limitations, however, use of such electrophysiological measurements has been used to study synchronized burst firing, a critical mechanism in development, and could lead to better platforms for anticonvulsant screening.^[142]

Calcium imaging and optical stimulation are also powerful tools to monitor neural activity in microfluidic devices.^[143] Channelrhodopsin-2 (ChR2) variants excited with blue light and Fluo-4 are popular candidates for optogenetic stimulation and calcium imaging respectively.^[144] These two modalities, however, have previously been incompatible because both have the same excitation frequency, thus limiting simultaneous stimulation and detection. To eliminate this problem, several ChR2 variants with red-shifted excitation peaks have been developed.^[145] Also, the use of orange-shifted calcium indicators in combination with ChR2 is another solution.^[146] The prospect of using electrophysiological techniques in microfluidic systems is promising for measuring synaptic plasticity, memory, and their importance in neurodegenerative diseases. Neuronal type, culture conditions, network topology, or stimulation patterns could be systematically examined to gain deeper insights into fundamental aspects of neuronal network behavior.

3. Modeling Neurodegenerative Diseases on a Chip

3.1. Brain on a Chip (CNS)

3.1.1. Neural Cell Culture Models

2D Compartmentalized Microfluidic Systems: CMSs have proven useful in the study neuronal behavior. They are composed of

multiple chambers separated by microgroove arrays and allow axon outgrowth into the microgrooves. The axons are spatially segregated from soma of neurons in these systems. Many studies have been performed using neuronal cultures to mimic the neuronal microenvironment in CMS using a microgroove system (Figures 2H, 4B,C, and 5A). This system enables isolation of the axons from the soma and dendrites of neurons by allowing axons to extend into the microgrooves. The axons reach the opposite chamber with this extension, often accelerated due to a hydrostatic pressure difference, and associated flow, between the two chambers.^[23,147] Cohen et al. studied BDNF-mediated dendrite-to-nucleus signaling and its related gene expression changes in a CMS. CMSs with short microgrooves (75 μm) facilitate fluidic isolation of neurites from soma and allow one to selectively expose dendrites to BDNF.^[148]

CMSs have been widely used as a model for intraneuronal (dendrites to axon) signaling, neuron–neuron interactions, as well as other cell interactions with neurons such as in studies of synapse formation/function, myelination, axon signaling, regeneration, and neuron–glial interactions.^[149] Taylor et al. developed a more advanced CMS to represent parts of the CNS. In this system, they manipulated neuron synapses between two neuronal populations by culturing neurons in two adjacent yet separated chambers (Figures 2H, 4B,C, and 5A). They characterized axon and dendrite growth within the microgrooves; axons outgrowth is extensive, far enough to reach the opposite chamber, while dendrite outgrowth is less so with thicker extensions. The synapses are visualized by immunocytochemistry staining of MAP2 and voltage-clamp recording.^[150] In a similar manner, Robertson et al. showed neuron–glia synapse formation in a CMS by co-culturing neuronal and glia cells in each of the separated chambers. Neurons and glial cells in each chamber grow within the microchannels where they physically interact and form synapses. The function of neuron–glia synapse was confirmed by calcium imaging.^[151] Yang et al. developed a co-culture CMS combined with electrodes to study activity-dependent myelination. They co-cultured neurons and oligodendrocyte and showed that electrical stimulation promotes the generation of myelin segments.^[152] In addition, there have been many other neuronal system studies in CMS including co-culture of axons with stem cells,^[153] osteoblasts,^[154] cardiomyocytes,^[155] and others.

Similar CMSs have also been used in the study of neurodegenerative diseases as an *in vitro* disease model. For instance, Kunze et al. studied the pathogenesis of ALS by co-culturing neurons and omission of second division 1 mutated astrocytes.^[156] One could explore uses of such microfluidic systems in the future to discover therapeutics for neurodegenerative diseases. The 2D-based CMS has the advantage of easy application of electrical and optical stimulation^[157] and easy quantification, for instance, by incorporating electrodes on the bottom of the chamber to quantitatively measure neuronal signals.

3D Hydrogel-Based Models: Microfluidic systems have been employed in the development of many brain-on-a-chip models by different groups using various concepts of 3D hydrogel encapsulation. For instance, Jang et al. mimicked 3D directional axonal growth in a 3D Matrigel-based hydrogel. An additional feature of this system was ECM alignment generated by

fluid flow. This group was one of the first ones to show that dendrites align parallel to the ECM fiber structure, introducing the potential to reconstitute a directional 3D neural network.^[158] They introduced a simple method to manipulate the 3D-aligned structure within an ECM hydrogel. With a more advanced design of the channel, the same group also mimicked the formation of an axon bundle that has 3D neuronal circuits within patterned Matrigel.^[159] Additionally, the microfluidic system incorporating an ECM hydrogel facilitated 3D co-culture of different cell types in the nervous system.

Studying cell–cell interactions in a physiological microenvironment are another useful application of 3D ECM-hydrogel-based culture systems. For instance, neuron–glial interactions have been studied in 3D by encapsulating neurons and glial cells in a patterned ECM scaffold in the microfluidic system. Wevers et al. developed a high-throughput system that enables patterning of the ECM-encapsulated cells in a microchannel with capillary pressure generated by a phase guide.^[160,161] They successfully formed neuron–glial networks in 3D by embedding neurons and astrocytes in the patterned Matrigel.^[161] Additionally, with this technique of 3D ECM patterning, the multilayered cortex was mimicked by alternating the patterning of neuron–hydrogel and neuron–free hydrogel under a chemical gradient of NGF.^[162]

Recently, many neurodegenerative disease models have been created by differentiating stem cells such as iPS cells and NSCs, and reconstituting them in a 3D microenvironment in a microfluidic system. This is a promising new technology to model neurodegenerative diseases. One particularly fascinating study involves the development of an AD model using differentiated stem cells.^[163] The AD model was created by culturing neurons differentiated from iPS cells derived from fibroblasts of a familial AD patient. Pathological events of AD are recapitulated by using neuronal cells expressing A β , differentiated from the neural stem cells engineered with multiple familial AD mutations.^[164] To regulate the cellular function and behavior of stem cells and to guide their differentiation, it is essential to understand the regulatory environmental factors that control stem cell fate.^[165]

Microfluidic systems, due to their microscale dimensions and flexibility, are well suited to capture the detailed behavior of neural tissues and to perform controlled studies of the various cell types involved. They also allow fine spatiotemporal control of biochemical and mechanical stimuli over elements of the cellular environment^[166] as described earlier. With these advantages of microfluidic systems, they have been employed by many researchers for stem cell studies, including those involving regulation of stem cell fate as a function of biochemical stimuli. The effect of growth factors or chemoattractants on growth and differentiation of NSC and iPS cells was studied by generating and maintaining a gradient of these biochemical factors across the microchannel using continuous flow or diffusion.^[20,167] This was used to apply different chemical stimuli to two sections of a single stem cell colony with the laminar flow of two parallel streams within the microchannel. This demonstrated the ability to induce different kinds (and levels) of differentiation^[168] and could be used to control the level of differentiation to a single cell type or for co-differentiation within a single stem cell colony.

ECM composition and the level of confinement (microfluidic vs Petri dish culture) also play a role as important regulators for stem cell fate as shown by Han et al. who developed a hydrogel-incorporated microfluidic system, which can provide an *in vivo* like microenvironment for NSC.^[169] Using this microfluidic system, they showed that the differentiation tendency of NSC depends on both the ECM composition and environmental level of confinement (micro/macro) by comparing differentiation fate of NSC cultured with various ECM compositions (Matrigel, collagen type 1, and a mixture of Matrigel and collagen type 1) and in various environmental confinements, respectively. Neuronal and oligodendrocyte differentiation was shown to depend on both the ECM composition and level of confinement. Specifically, neuron and oligodendrocyte differentiation was enhanced in Matrigel and in the mixture of Matrigel and collagen type 1 in a microfluidic system. But astrocyte differentiation exhibited no dependency on either matrix composition or confinement.^[169] Hesari et al. also showed that neural differentiation of human iPS cell is enhanced when they are cultured in a 3D microenvironment reconstituted within the microfluidic system, compared to those cultured on culture dishes.^[170]

Co-culture with support cells could also influence stem cell fate. For instance, the viability of NSC and iPS cells is enhanced, and their differentiation is regulated in the presence of support cells. To demonstrate this, studies were performed in a 3D co-culture microfluidic system, which enables spatial patterning of different types of cell in well-defined regions. In one case, a 3D co-culture system was developed to reconstitute a 3D vascular microenvironment that allowed close interaction between NSC and the vascular network.^[29] The NSC viability and self-renewal ability were improved, and astrocyte differentiation was increased in co-culture with brain endothelial cells.

3.1.2. Neurovascular Unit and BBB

The BBB has structurally and functionally specialized properties, acting as a functional, selective barrier with low permeability in order to protect the brain from harmful substances entering from the blood vessels. This property is essential to ensure and maintain the normal function of the CNS. The BBB is composed of microvascular endothelium surrounded by astrocyte foot process and pericytes embedded within a basement membrane. The endothelium of the BBB has low permeability compared to that of the endothelial lining in other organs. This low permeability also correlates with high expression of tight junction proteins such as ZO-1, claudin, and occludin, and a selective transport system regulated by the number of influx and efflux transporters such as P-glycoprotein (P-gp) and the receptor for advanced glycation end products (RAGE).^[49,171]

Emerging studies show that the BBB is implicated in the pathogenesis of neurodegenerative diseases such as AD, PD, and Huntington's disease, and a primary determinant of drug delivery to the brain.^[59,172] Dysfunction of the BBB such as an increase in permeability appears in AD and PD patients, suggesting a possible role for BBB disruption in these diseases. The BBB is also affected in disorders such as cerebral amyloid angiopathy. As the importance of the BBB in the neurodegenerative

disease continues to emerge, the need for a BBB model has also been increased. In order to better understand the pathological mechanisms of several neurodegenerative diseases and to develop therapeutic drugs, it is therefore important to develop a BBB model that closely emulates *in vivo* physiology.

Current *in vitro* BBB models rely primarily on a 2D monolayer with a traditional assay, such as the Transwell system, in which bECs are cultured in a monolayer on top of a microporous semipermeable membrane. These Transwell systems have a vascular and an adluminal compartment (top–bottom) with vertical diffusion of biochemical factors across the membrane and endothelial layer. This BBB model is a high-throughput system to measure drug transport and binding affinity and could be used for not only monocultures of ECs but also for co-cultures of neuronal cells in the bottom compartment.^[173] However, the limitations of a simple Transwell system have constrained its capacity to mimic important features that are necessary for reconstituting BBB properties.

In traditional Transwell systems, it is difficult to precisely control microenvironmental factors or to obtain quantitative results in real time. To overcome these limitations, a promising approach has recently been introduced to develop microfluidic-based BBB models that can provide a more physiologically relevant microenvironment with mechanical and chemical stimuli that simultaneously allow straightforward monitoring with potential for quantitative evaluation. These BBB-on-a-chip models have been developed with various cell sources and design concepts for a range of applications (Table 1).

Many monolayer-based BBB-on-a-chip systems have been proposed. Typically, these consist of a porous membrane on which a monolayer of bECs is formed and multiple chambers on either side of the membrane which could have continuous perfusion and/or the culture of other neural cells (Figure 3A). Such designs are useful for applying continuous perfusion, shear stress, and the measurement of TEER for quantifying permeability. Hence, many researchers have applied it to reconstitute an *in vitro* BBB model and demonstrate BBB function. For example, Griep et al. developed a microfluidic system that is composed of two layered chambers with a porous membrane in between. They formed a monolayer of bEC (hCMEC/D3, a human brain microvascular endothelial cell line) on the membrane, applied a shear stress on the bEC monolayer, and confirmed that this shear stress increased the expression level of tight junction proteins in the bECs with a consequent decrease in permeability.^[181]

The system has also been used for co-culturing bEC with neural cells to mimic more physiologically relevant features of the BBB. Achyuta et al. demonstrated a neurovascular unit by co-culturing bEC (RBE4: rat brain endothelial cell line) on the porous membrane in the upper channel and neuron–glia cells in the bottom channel (Figure 3A). Because of different maturation periods of bEC and neuron–glial cells, they were cultured separately, and then the two chambers were assembled to enable communication through the porous membrane.^[184] Wang et al. mimicked *in vivo* like BBB integrity and permeability by co-culturing iPS cell-derived brain microvascular endothelial cells and astrocytes on the porous membrane of the bottom chamber side and on the upper chamber side, respectively (Figure 3B).^[192] They introduced a “step chamber” in the

Table 1. The BBB model in a microfluidic device.

Ref.	Device fabrication	Endothelial cells	Co-culture cells	Physiological function	Results	Permeability measurements	TEER	Shear stress
Adriani et al. (2017) ^[131]	3D single layer PDMS-device with two channels	Green fluorescent protein (GFP)-Human umbilical vein endothelial cell (HUVEC)/ hCMEC/D3	Primary brain astrocytes	N.A.	N.A.	6.58×10^{-5} to $3.3 \times 10^{-6} \text{ cm}^2 \text{ s}^{-1}$	N.A.	N.A.
			Rats cortical neurons E18			10 and 70 kDa dextran, 4 and 7 d culture		
Herland et al. (2016) ^[132]	3D PDMS device viscous fingerprinting procedure	Human brain microvascular endothelial cells (hBMVEC)	Human brain pericytes	TNF- α -mediated inflammation	G-CSF and IL-6. IL-8 release increased compare to static Transwell culture and between co-cultures	$2-5 \times 10^{-6} \text{ cm}^2 \text{ s}^{-1}$	N.A.	100 mPa
			Human brain astrocytes			3 kDa dextran		
						Different co-culture systems		
Wang et al. (2017) ^[174]	3D-printed microfluidic chamber	hiPS-derived BMEC	Primary rat astrocytes	Exposure to small drugs molecules (caffeine, cimetidine, doxorubicin)	Permeable to molecules	4, 20, 70 kDa dextran	2000–4000 $\Omega \text{ cm}^2$	2–3 mPa
Cho et al. (2015) ^[175]	3D PDMS composite assembly of horizontal parallel microchannel beside one macrochannel	Rat brain endothelial cells (RBE4)	Human neutrophils	Neutrophils transmigration	Inhibition of neutrophils transmigration	10^{-7} – $10^{-8} \text{ cm}^2 \text{ s}^{-1}$ 40 kDa, visual diffusion comparison	N.A.	N.A.
				TNF- α -mediated	Neuroinflammation response			
				Inflammation Oxygen–glucose deprivation-Antioxidant treatment	Reactive oxygen species (ROS) and Rho-associated protein kinase (ROCK) activation Cell death Limited antioxidant effect			
Deosarkar et al. (2015) ^[176]	PDMS circular device independent vascular channel	Rat brain endothelial cells	Neonatal rat astrocytes	N.A.	N.A.	40 kDa under flow condition: $41-1.1 \times 10^{-6} \text{ cm}^2 \text{ s}^{-1}$ for co-culture condition	N.A.	0.38–7.6 mPa
Wang et al. (2016) ^[177]	Two-layered microfluidic channel's porous membrane	Mouse brain endothelial cells (b.End3)	Mouse astrocyte (C8D1A)	P-gp efflux pump functional expression by dexamethasone	Increased by culture days, P-gp expression in mono co-cultures	Urea, 1.1×10^{-6} Mannitol, $0.3-0.6 \times 10^{-6} \text{ cm}^2 \text{ s}^{-1}$	320 $\Omega \text{ cm}^2$	160 mPa
			Immortalized mouse pericytes			Dexamethasone 2.9×10^{-6} permeability		
Brown et al. (2015) ^[178]	3 PDMS layers 1 polycarbonate filter membrane	Human brain microvascular endothelial cells (hBMVEC)	Primary human brain pericytes	Exposition to glutamate ascorbate	Increased permeability to ascorbate	24 h fluid flow of 10, 70 kDa dextran	5–30 $\text{k}\Omega \text{ cm}^{-2}$	2 mPa
			Primary astrocytes Human cortical glutamatergic neurons from hiPSCs	Cold shock	Disruption of Tight junctions (TJs) TEER decrease	Compare diffusion across the membrane		
Kim et al. (2015) ^[179]	3D-printed collagen gel and channels	Immortalized mouse brain endothelial cells (b.end3)	N.A.	BBB disruption by hyperosmotic D-mannitol exposure	Increase of permeability	40 kDa dextran-	N.A.	N.A.

Table 1. Continued.

Ref.	Device fabrication	Endothelial cells	Co-culture cells	Physiological function	Results	Permeability measurements	TEER	Shear stress
					And recovery after treatment	$2.27 \times 10^{-7} \text{ cm}^2 \text{ s}^{-1}$		
						$6.5 \times 10^{-10} \text{ cm}^2 \text{ s}^{-1}$		
						Mannitol $3.9 \times 10^{-6} \text{ cm}^2 \text{ s}^{-1}$		
Booth et al. (2012) ^[180]	PDMS sublayer Polycarbonate membrane	Immortalized mouse brain endothelial cells (b.end3)	C8D1A astrocytes	Histamine exposition	Response after histamine, recover TEER initial value in 6–15 min	4, 20, 70 kDa Propidium iodide	50–280 $\Omega \text{ cm}^2$ 10–25 $\Omega \text{ cm}^2$ in Transwell	0.08 mPa co-culture
Griep et al. (2013) ^[181]	Two-layered membrane-based device made of PDMS polycarbonate membrane	hCMEC/D3	N.A.	TNF- α -mediated inflammation under stress	TNF- α and mechanical stimulation have more impact compared to Transwell on TEER	N.A.	40 $\Omega \text{ cm}^2$ under shear stress 120 $\Omega \text{ cm}^2$ TNF- α under shear stress 12 $\Omega \text{ cm}^2$	580 mPa
Partyka et al. (2017) ^[182]	1 hydrogel reservoir up on two microchannels	hCMEC/D3	Human astrocytes	TNF- α -mediated inflammation with and without shear stress	Permeability increase in co-cultures	4 kDa dextran -Flow $0.6\text{--}1.2 \times 10^{-6} \text{ cm} \text{ s}^{-1}$ -TNF- α $4\text{--}9 \times 10^{-6} \text{ cm} \text{ s}^{-1}$	Static 180–220 $\Omega \text{ cm}^2$ Flow 220–1000 $\Omega \text{ cm}^2$	50 mPa
Prabhakarpandian et al. (2013) ^[183]	Circular PDMS device	Rat brain EC RBE4	N.A. (Astrocyte conditioned media (ACM))	P-gp efflux activity	Reduction of P-gp in the presence of verapamil	3, 5 kDa comparison with ACM	N.A.	3 mPa
Achyuta et al. (2013) ^[184]	2 PDMS chamber and polycarbonate membrane	Rat brain EC RBE4	E18 neural cells Differentiate into neurons, astrocytes, microglia	TNF- α mediated Inflammation	Hyperpermeability TNF- α induced	3 kDa dextran Relative comparison	N.A.	N.A.
					ICAM-1 and glial activation			
Yeon et al. (2012) ^[185]	Two-channel PDMS device	HUVEC	N.A. (Astrocyte conditioned media (ACM))	Effect of ACM and hydrogen peroxide on endothelial permeability	Increase of permeability	4, 40, 70 kDa relative comparison	N.A.	N.A.
Walter et al. (2016) ^[186]	PDMS–polyethylene terephthalate (PET) membrane–glass device assembly	hCMEC/D3 or primary rat brain endothelial cells	Primary brain pericytes Primary brain astrocytes	N.A.	N.A.	Sodium fluorescein 376 Da dextran 4.4 kDa Evans blue-labeled albumin 67 kDa $0.4\text{--}1.57 \times 10^{-6} \text{ cm} \text{ s}^{-1}$	Static 10–20 $\Omega \text{ cm}^2$ Dynamic 19–30 $\Omega \text{ cm}^2$	150 mPa
Sellgren et al. (2015) ^[187]	Two-compartment PDMS device and Polytetrafluoroethylene (PTFE) membrane	Murine brain endothelial (b.end3)	Astrocytes (C8D1A, ATCC)	N.A.	N.A.	Dextran 70 kDa, $6 \times 10^{-7} \text{ cm} \text{ s}^{-1}$	N.A.	500 mPa

Table 1. Continued.

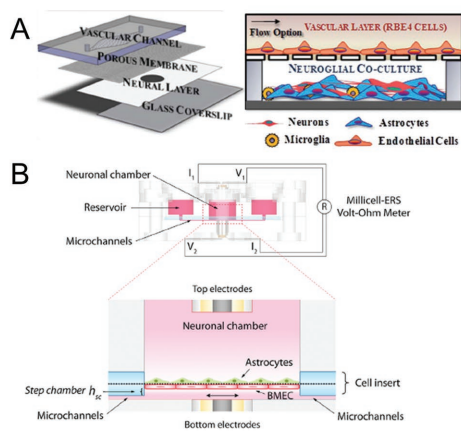
Ref.	Device fabrication	Endothelial cells	Co-culture cells	Physiological function	Results	Permeability measurements	TEER	Shear stress
Labus et al. (2014) ^[188]	Transwell inserts with 3.0 μm pore polycarbonate membranes	Transfected human brain microvascular endothelial cells	Leukocytes Peripheral blood mononuclear cells (PBMCs)	TNF- α , IL-1 β -mediated neuro inflammation transmigration of PBMCs after neuroinflammation	Increase of ICAM-1 MMP's expression -Reduction of ZO-1 and occludin -Increase of PBMCs transmigrated	Sodium fluorescein, $1 \times 10^{-6} \text{ cm s}^{-1}$	250 $\Omega \text{ cm}^2$	N.A.
Thomsen et al. (2015) ^[189]	Cell culture insert	Porcine brain endothelial cells (PBECS)	Cerebral porcine pericytes porcine glia cells (mainly astrocytes) rat astrocytes rat pericytes	N.A.	N.A.	6×10^{-5} to $0.8 \times 10^{-6} \text{ cm s}^{-1}$	70–1800 $\Omega \text{ cm}^2$	N.A.
Nakagawa et al. (2008) ^[190]	Transwell inserts polyester membrane	Primary cultures of rat brain capillary endothelial cells	Rat cerebral astrocytes Rat cerebral Pericytes	Activity of P-glycoprotein By transport of rhodamine 123 and drug transport	Different transport rate	$3 \times 10^{-6} \text{ cm s}^{-1}$	400 $\Omega \text{ cm}^2$	N.A.
Merkel et al. (2017) ^[191]	Cell culture insert PET membrane 0.3 μm	hBMVEC isolated from temporal of hippocampal tissue	Human primary astrocytes	Comparison of adeno-associated virus vectors AAV9 AAV2 Trafficking the BBB	AAV9 more efficiently cross the barrier AAV9 does not affect TEER, permeability, TJs' expression	3 kDa dextran 16 000 RU 40 kDa dextran 800 RU	1000–1240 $\Omega \text{ cm}^2$	N.A.

bottom to minimize shear stress on the ECs, in order to establish that a minimal shear stress (lower level than other studies) enhances BBB integrity in BBB-on-a-chip models. The monolayer-based BBB-on-a-chip models have several advantages including the ease of application of perfusion flow and the ease of electrode integration for the quantitative analysis of permeability using TEER. However, there are still some limitations, such as the 2D geometry of the culture, which prevent it from better mimicking physiologically relevant 3D physical features of the BBB.

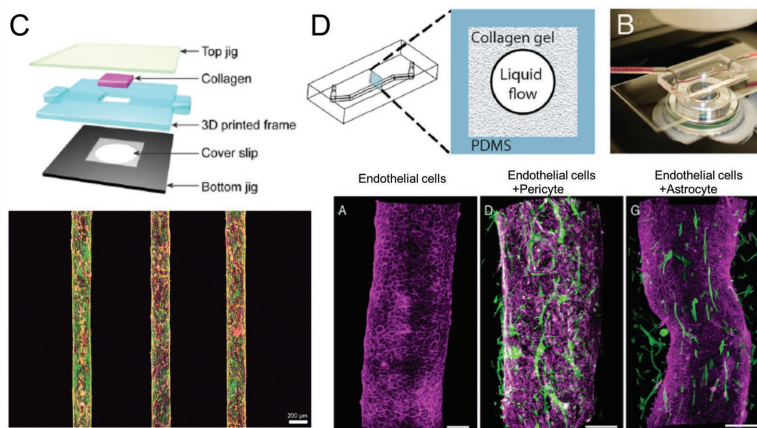
Microfluidic systems with designs that permit integrating a 3D ECM scaffold provide an opportunity to overcome this limitation. Such an ECM hydrogel scaffold provides a 3D physical tissue microenvironment that significantly helps maintain BBB function. Various methods have been developed to more closely mimic the features of the BBB such as incorporating appropriate cell–cell interactions (bEC with pericytes or astrocytes), cell–ECM interactions, and appropriate geometrical constraints (cylindrical geometry). Kim et al. developed a cylindrically shaped BBB model embedded in a collagen scaffold by combining 3D printing and microfluidics (Figure 3C).^[179] They fabricated a frame for encasing a collagen scaffold using 3D printing. Then, microneedles were inserted manually into

the 3D printed frame, and collagen solution was introduced. After collagen polymerization, the microneedles were removed and then bECs were seeded into the cylindrical channels. This method allowed bECs to line the inner wall of the cylindrical channel, which is similar to their natural physiological form in the BBB. Herland et al. used a different approach, forming a 3D cylindrical lumen in a hydrogel by taking advantage of the viscous fingering instability (Figure 3D).^[132,193] After forming the lumen scaffold structure, cortex-derived human brain pericyte and human brain microvascular endothelial cells (hBM-VECs) were sequentially seeded into the channel. They then co-cultured astrocytes by embedding them in 3D in the hydrogel. This group showed that the permeability of the vascular-like structure was reduced even further when either astrocytes or pericytes were co-cultured with the endothelial cells, with co-cultures synergistically improving barrier function under perfusion. They also showed the neuroinflammatory response such as granulocyte-colony stimulating factor (G-CSF) and IL-6 in vitro by adding TNF- α . Overall, they claimed that there is a significant advantage in using their model over Transwell models for studies of neuroinflammation. This was postulated to be a consequence of the G-CSF, an important neuroprotective cytokine^[194] secreted in response to brain injury by endothelial

i) 2D Monolayer based BBB model



ii) Lumen-shaped BBB model



iii) Lumen-shaped BBB model with neural cells

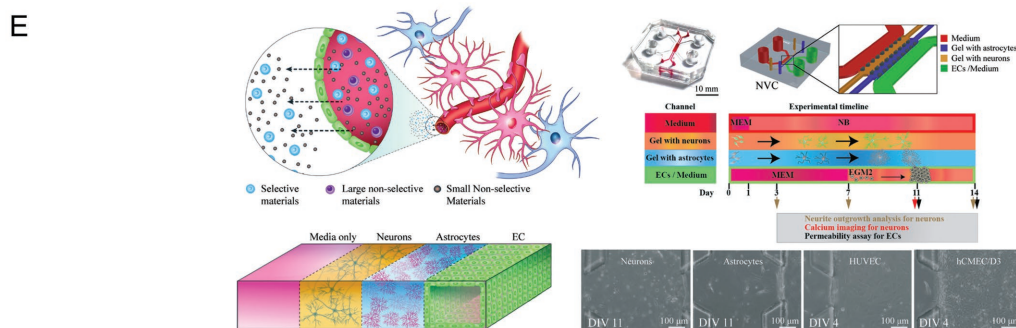


Figure 3. In vitro models of BBB. A) A 2D monolayer based neurovascular unit-on-a-chip. The system consists of two main chambers separated by a porous membrane. A neurovascular co-culture was performed by assembling vascular and neural culture chambers after vascular monolayer formation and neuronal differentiation was separately performed. Reproduced with permission.^[184] 2013, The Royal Society of Chemistry. B) A BBB-on-chip equipped with the electrodes for TEER measurement. The system enables physiologically relevant luminal perfusion past the BBB monolayer, minimizing the shear stress magnitude by introducing a “step chamber”. Reproduced with permission.^[192] C) A collagen-based cylindrical BBB microvascular model. The cylindrical shape of BBB was performed by introducing microneedles within the collagen scaffold in the 3D-printed frame. After removing the microneedles, bECs were seeded into the collagen microchannels to form a lumen-shaped BBB. Reproduced with permission.^[179] 2015, AIP Publishing LLC. D) A 3D BBB model was developed by fabricating a cylindrical hollow region within a collagen scaffold driven by viscous fingering. bECs were then seeded into the hollow channel to form a lumen-shaped structure. Also co-culturing with pericytes and astrocytes was performed by plating pericytes on the luminal surface of the gel prior to bEC seeding and embedding astrocytes in the surrounding gel. Reproduced with permission. 2016, Public Library of Science. E) A 3D neurovascular microfluidic model. The system consists of four channels, two side channels for media supplement and two center channels for 3D neuron and astrocyte culture. The neurovascular unit was reconstituted by culturing neurons and astrocytes in each hydrogel channel and forming a bEC monolayer in the side channel. Reproduced with permission.^[131] 2017, Royal Society of Chemistry.

cells, astrocytes, and neurons,^[195,196] and promoting neuronal survival and proliferation^[197] in AD patients.

Recently, our group developed a new microfluidic platform that combined the compartmentalization capabilities of previous 2D models with a 3D ECM scaffold. This system was used to investigate the interaction between cerebral endothelial cells, neurons, and astrocytes by culturing the three cell types together in separate channels in a microfluidic device to produce a neurovascular chip (Figure 3E).^[131] This platform was used to measure permeability across two types of endothelial cells, with or without neurons and astrocytes, and to test how chemical compounds cross the endothelial barrier. The endothelial barrier formed by human cerebral microvascular endothelial cells (hCMEC/D3) exhibited low permeability to three different molecular weights of dextrans compared to the corresponding permeabilities of human umbilical vein

endothelial cells. Furthermore, unlike previous systems, this device could also be used to study detailed cellular dynamics through high-resolution imaging.

As discussed above, changes in the BBB function are closely related to the pathology of neurodegenerative diseases. Thus, a well-validated BBB-on-a-chip technology would be well suited not only to the study of pathological mechanisms of neurodegenerative disease but also to the development of new methods of therapeutic drug delivery.

3.1.3. Alzheimer's Disease Models

AD is a progressive neurodegenerative disorder, which is characterized by two pathological features—A β plaques and neurofibrillary tangles—that are thought to cause brain damage.^[198]

The amyloid hypothesis suggests that the extraordinary accumulation of $A\beta$ within brain is a trigger and the primary event of AD pathogenesis. This has been the main theory that the AD research community has adopted for AD pathological mechanisms over the last two decades. However, recently Alzheimer's drugs targeting the removal of $A\beta$ plaques, based on the amyloid hypothesis, have failed in clinical trials. This has led to an urgent need for the development of in vitro human AD models in order to study AD, develop a comprehensive understanding of the complex mechanisms of AD pathogenesis, and finally test therapeutic drugs.

Many studies have shown that the BBB and inflammation have key roles in AD pathogenesis and therapeutic drug delivery. Several groups have shown that dysfunction of BBB is associated with AD and it seems to increase the risk of AD. Therefore, there has been an increasing recognition that the BBB and the immune system have an important role in AD. Recent studies have identified BBB leakage in patients with early-stage AD, and there is some evidence to suggest that this may be a cause of AD pathogenesis. The typical characteristics of BBB dysfunction in AD include a BBB permeability increase, decrease of tight junction protein expression, and disruption of the $A\beta$ clearance system. Even though many studies have been conducted to elucidate the mechanisms behind BBB changes in AD, the exact cause of BBB dysfunction in AD has not yet been identified. Some researchers have shown that $A\beta$ -40 and $A\beta$ -42 affect BBB leakage by degrading the expression of tight junction proteins and increasing the expression of MMP-2 and MMP-9. Interaction between $A\beta$ -42 and RAGE is also associated with disruption of tight junction proteins. Additionally, other studies have shown that the degradation of pericytes and astrocytes by $A\beta$ -independent effects of apolipoprotein E could lead to a loss of BBB function.

Many studies over the past decade have brought the fundamental role of neuroinflammation in AD pathology to the forefront. Inflammatory players in AD pathogenesis include microglia and astrocytes, which are activated by $A\beta$ and produce pro-inflammatory molecules including cytokines such as IL-1, IL-6, and TNF- α . It was reported that a significant increase in pro-inflammatory molecules causes neuronal damage and might influence amyloid deposition.^[199] Also, it was recently reported that microglia play a role in converting aggregated $A\beta$ into neurotoxic forms.^[200] Therefore, in addition to reconstruction of neuronal networks, incorporating changes in the BBB as well as inflammation is necessary in creating a comprehensive AD model.

Traditional in vitro human AD studies using simple Petri-dish-based cultures are insufficient. Most of these studies have been performed by observing neuronal death through $A\beta$ -induced damage. These studies used neural cells cultured either on a 2D substrate or in a 3D ECM hydrogel and tested their response to $A\beta$. Many in vitro AD models have been developed by using patient-derived neurons, neurons differentiated from neural stem cells with the Familial Alzheimer's disease (FAD) mutation, or from iPS cells. With advanced technologies, 3D AD models recapitulating the generation of $A\beta$ plaques or neurofibrillary tangles have been successfully developed. With these 2D cell cultures, we are limited in our understanding of

the mechanisms of AD pathology including AD-related BBB dysfunction and inflammation as well as neural damage.

Transwell-based systems could be used to model more complex features of AD. Studies of AD-related BBB dysfunction using such systems have been underway for over two decades. Such studies are typically conducted by culturing bECs as a monolayer on porous Transwell membranes and investigating their response to $A\beta$ exposure. In these systems, BBB dysfunction is evaluated both by observing changes in expression levels of tight junction proteins or $A\beta$ mediating transporters and by measuring changes in the permeability. The AD–inflammation link has also been studied in a similar manner. $A\beta$ -associated microglial activation was studied by culturing microglia on well plates and treating them with $A\beta$. Activation of microglia is evaluated by observing morphological changes or signaling activation.^[201]

The Petri dish and Transwell models are both traditional AD models that have led to many discoveries. However, they are unrealistic in terms of how they mimic the complex features of AD pathology. They lack a number of critical in vivo like physiological features as well as controlled physical stimuli^[202] such as direct cell–cell interactions, controlled flow dynamics, circulating blood cells, and a brain-specific microenvironment and ECM.

Several in vitro AD models have been developed in microfluidic systems to tackle some of the limitations of these traditional AD systems. Studies of $A\beta$ toxicity on neural networks and transmission have been performed by many groups. Choi et al. investigated the neurotoxicity of $A\beta$ oligomeric assemblies by developing a microfluidic platform capable of generating a gradient of $A\beta$ oligomeric assemblies within microchannels.^[203] They induced an osmotic pressure to generate a slow flow similar to the interstitial flow in brain by incorporating an osmotic pump into the platform. Neuronal cells adhered to the microchannel were exposed to a gradient of $A\beta$ oligomeric assemblies, and their neurotoxicity was evaluated by the Live/Dead assay, immunocytochemistry staining, and Fluorescence-activated cell sorting (FACS) analysis. Park et al. from the same group extended this work to develop a 3D AD model in a microfluidic system incorporating 3D neurospheres more closely mimicking the brain tissue (**Figure 4A**). To test $A\beta$ neurotoxicity, 3D neurospheres were exposed to $A\beta$ via an osmotic pump in the same way.^[204] Deleglise et al. investigated the pattern of neuronal degeneration by $A\beta$ peptide by using a CMS.^[205] Soma–dendrites and axons are separated in each fluidically isolated chamber which permits treating each cell type with $A\beta$ peptide separately. This study found that soma–dendrites are associated with $A\beta$ peptide-induced synaptic loss, but axons are not. Song et al. also demonstrated $A\beta$ transmission via neuronal networks that might contribute to the spreading of plaque that occurs in neurodegeneration.^[206] They used a CMS composed of three main culture chambers, connected by arrays of microgrooves, enabling synapse formation. Within the system, they demonstrated transneuronal and retrograde $A\beta$ transmission from axons to cell bodies, suggesting that blocking $A\beta$ transmission may be a useful therapeutic approach. In addition, neuron-to-neuron tau propagation was examined within a CMS. A CMS composed of three chambers was also used to model the synaptic connections by forming dual layered

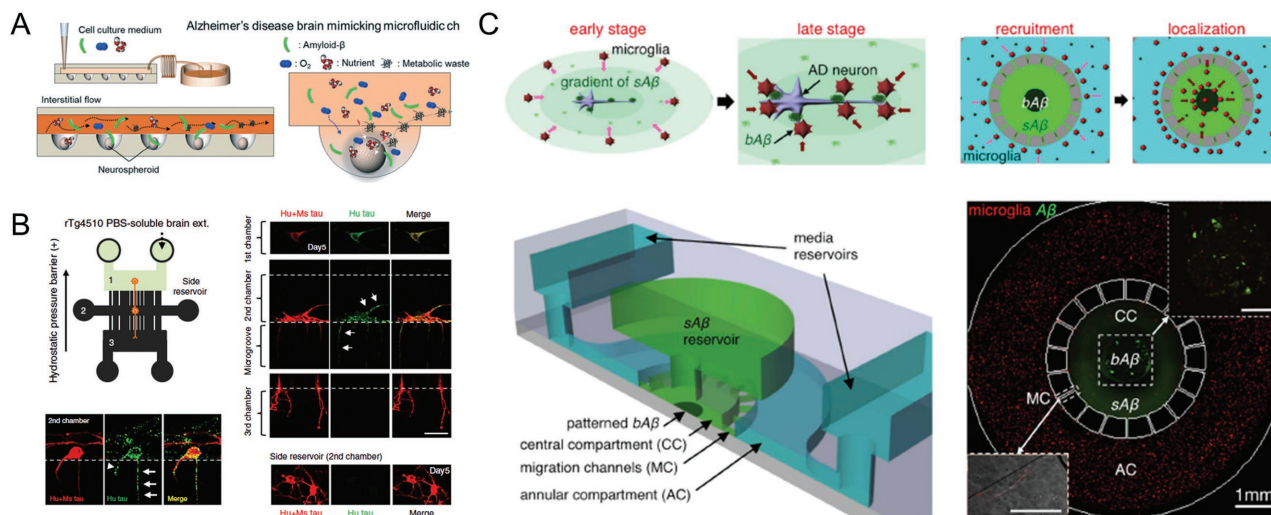


Figure 4. In vitro model of Alzheimer's disease. A) A hydrogel free neurospheroid-based AD model. Neurospheroids were formed in a microfluidic system containing concave microwells with an interstitial flow driven by an osmotic pump. To study neurotoxicity of $A\beta$ of the AD, the neurospheroids that were cultured in the system were exposed to medium containing synthesized $A\beta$ and evaluated with a Live/Dead assay. Reproduced with permission.^[204] 2015, Royal Society of Chemistry. B) A microfluidic study of tau propagation from neuron to neuron. The system is composed of three main chambers connected by arrays of microgrooves. Axon growth and synaptic formation were performed by seeding neurons in the first and second chambers and allowing axon isolation from soma and dendrites. Tau transfer is confirmed by detecting tau positive axons in the third chamber after 14 d of tau treatment in the first chamber. Reproduced with permission.^[206] 2015, Macmillan Publishers. C) A microfluidic platform to study microglial responses to various types of $A\beta$. The system is composed of two chambers connected by microchannels, which enable generation of a long lasting gradient of soluble $A\beta$. The system also features patterning of the $A\beta$ on the bottom. A range of different behaviors of microglia are observed in response to different types of $A\beta$. The microglia migrate along the gradient of soluble $A\beta$ but their speed slowed on the patterned $A\beta$, where they were also found to accumulate. Reproduced with permission.^[208] 2013, Nature Publishing Group.

neurons to investigate tau transfer (Figure 4B).^[207] High-molecular-weight tau was added in the first compartment that contains the soma and dendrites of the first layer of neurons, and its propagation into the axons in the third chamber via the synaptic connections in the second chamber was observed with time-lapse analysis.

In addition to studies involving the direct influence of $A\beta$ neurotoxicity or tau on neural networks, the role of neuro-inflammation in AD pathology has also been studied in microfluidic systems. Cho et al. investigated the migration and accumulation of microglia under a chemotactic gradient of $A\beta$ using a microfluidic system (Figure 4C).^[208] They reported that under gradients of soluble $A\beta$, microglial morphology first changes followed by migration toward the chamber with soluble $A\beta$. This group also performed studies on $A\beta$ fibril-coated surfaces. They found that the microglial motility was decreased specifically in areas on the surface that were patterned with $A\beta$. When the surface-patterned $A\beta$ and the soluble $A\beta$ were combined, there was a synergistic effect on microglial accumulation. Bianco et al. developed a microfluidic system that enables investigation of the mechanisms of cellular interactions between astrocytes and neurons during neuro-inflammatory events.^[209] They found that astrocytes from the hippocampal (but not cortical) area of the brain have a detrimental role on neurons when exposed to $A\beta$ fibrils. This study brings up the importance of incorporating astrocytes in modeling AD pathogenesis.

Even though BBB dysfunction plays a key role in AD, there have been a few well-controlled microfluidic studies in this area. One advantage of a 3D microfluidic-system-based BBB

model is that it enables studies of various aspects of BBB-related pathological phenomena in AD. For example, changes in BBB permeability under treatment with $A\beta$ - or AD-related chemokines could be visually observed. Well-controlled cell–cell interactions can be studied by co-culturing $A\beta$ neurons along with a BBB model composed of endothelial cells with astrocytes and pericytes, all in the same complex microfluidic system. Such systems could also facilitate real-time monitoring of physical and chemical events between cells.

3.1.4. Parkinson's Disease and Huntington's Disease Models

PD is a progressive disorder characterized by the loss of dopaminergic neurons in substantia nigra pars compacta along with the abnormal aggregation of intracellular proteins such as α -Syn.^[210] The symptoms of PD include uncontrollable tremors, postural imbalance, and slowness of movement and rigidity.^[211] α -Syn is the major component of Lewy bodies that develop inside both nerve cells and filamentous inclusion characteristics of PD as well as are found in other synucleinopathies such as Lewy bodies dementia and multiple atrophy. The aggregated α -Syn in these Lewy bodies is thought to play a role in neurodegeneration. It has been hypothesized that aggregated α -Syn might behave like a prion, which is an infectious agent composed entirely of protein material, capable of initiating misfolding and aggregation of nascent or even properly folded α -Syn.^[212,213] Analysis of the production and aggregation of α -Syn as well as its crystallographic structure is necessary for a thorough investigation of axon–glia interactions^[69] in addition

to developing appropriate co-culture systems with dopaminergic neurons, oligodendrocytes, and astrocytes.

To date, there are a few realistic *in vivo* like models for PD. Some of the current models include the one by Freundt et al.^[214] in which they demonstrate a culture model of primary neurons in the presence of fibrils of α -Syn in microfluidic devices with microgrooves. They showed that α -Syn fibrils are internalized by neurons and transported along the axons. This transfer of α -Syn fibrils to neuronal somata is similar to the characteristic pattern of spread of Lewy bodies. In order to make these models more relevant to PD pathophysiology, one could integrate α -Syn transport tracking with compartmentalized microfluidic systems and PD patient-derived cells. Compartmentalized chambers for neuron patterning would allow quantitative analysis of neural activity to investigate the pathogenesis of PD. Such models could be made even more realistic by adding novel microfluidic features such as integration of microvalves to control fluid routing and reconstitution of paracrine signaling between the various neural cells.

Huntington's disease is an inherited neurological disorder caused by an expansion of cytosine-adenine-guanine (CAG) trinucleotide repeats in the gene encoding the Huntington's protein (Htt). It is estimated to affect 7–10 individuals per 100 000 and is most prevalent in populations of European origin.^[215] Htt expression is involved in numerous biological processes, such as in regulating neural cell apoptosis,^[216] in enhancing microtubule-based transport, and in scaffolding of cytoskeletal molecules at synapses.^[217] Htt also induces abnormal gene expression,^[218] aberrant protein folding, degradation and clearance, and the formation of large protein aggregates called inclusion bodies.

Successful models of HD in culture rely on the ability to differentiate iPSCs or ESCs into inhibitory GABAergic medium spiny neurons including other affected cell types, such as cortical neurons, astrocytes,^[219] and possibly oligodendrocytes expressing Htt. It has been demonstrated that iPSCs can successfully be derived from individuals with severe neurodegenerative disorders, and these patients display robust phenotypes that replicate many features of their respective diseases, carrying all of the associated genetic components that make certain cell types susceptible to a disease state.^[220] In the case of HD, the use of iPSCs^[221] is a fundamental innovation that allows researchers to study the most genetically precise model of the disease.^[222]

So far, developing a realistic HD model has been particularly challenging because the mechanism of HD pathogenesis is largely unknown compared to AD or PD. To facilitate our mechanistic understanding of HD, we should develop realistic *in vitro* cell culture models for the disease process. However, cells growing in a Petri dish lack many critical features of neural cells that have developed *in vivo*. First, the complex brain microenvironment including the mechanical and chemical cues may be important to fully reproduce and understand how Htt alters cellular function. Second, there are many other cell types within the brain other than neurons that contribute to the pathological processes of neurodegenerative diseases. The contribution of each cell present in the brain may be studied in precisely defined co-cultures in microfluidic platforms. Despite the promise of microfluidic technology for modeling complex

neurodegenerative diseases such as HD, no 3D microfluidic models of HD are reported in the literature.

An important factor in HD progression is the potential role of aging in neurodegeneration. As the symptoms of HD typically emerge in late adulthood, years rather than weeks of Htt expression may be necessary to fully replicate the disease.^[223] Moreover, it is possible that the disruption of cellular function by Htt may be offset more readily in young versus aged cells in a way such that symptoms may only present themselves in late adulthood. For this reason, it would be interesting to develop long-term cell cultures with Htt.

3.1.5. Prospective Works for Brain-On-a-Chip

An integrated model of the brain would be a tremendous aid to our understanding of the pathogenesis of brain-related diseases such as AD, PD, and HD as discussed in this review, as well as after injuries such as cerebral infarction and subarachnoid hemorrhage. To realize a brain-on-a-chip, the co-culture of various types of cells specific to the brain would be important. In particular, stem cells derived from adipose tissue and bone marrow as well as iPS cells could potentially be used to generate these cells. In studies of the use of iPS cells for tailor-made treatments and drug screening, one long-standing problem has been the lack of effective differentiation protocols to obtain mature bECs from iPS cells (as they are very specialized). However, in 2017, Yamamizu et al. solved this problem by inducing mature bECs from iPS cells. Their protocol involved co-culturing iPS endothelial lineage cells with iPS-derived pericytes, neurons, and astrocytes.^[133] They found that the Notch signaling pathway (between the endothelial lineage cells and iPS neurons) was involved in this fate specification. Although this is a breakthrough development, this differentiation is a process that is quite cumbersome and expensive. Monolayers made from these induced bECs have permeabilities that correlate well with the BBB permeability reported previously. They also have a high expression of specific transporters for brain endothelial cells such as high expression of nutrient transporters (CAT3 and MFSD2A) and efflux transporters (ABCA1, BCRP, PGP, and MRP5).

In order to further investigate neurodegenerative disorders and develop *in vitro* models that could be applied in drug screening, we think it is necessary to combine all our biological mechanistic and process-oriented knowledge (efficient differentiation procedure of iPS cells and cost-effective methods) along with the fabrication of appropriate microfluidic devices to reconstitute the microenvironment of brain. In particular, because the development of AD is related to endothelial function and dysfunction, which in turn is sensitive to various mechanical stresses, microfluidic platforms occupy an important role for further progress in this field.

Brain organoids have emerged as an alternative to using engineered bottom-up platforms as brain models. Lancaster et al. have shown the possibility of engineering 3D brain organoid from iPS cells.^[224] They cultured the neuroectoderm tissue embedded in droplets of Matrigel (as scaffolds) to support complex tissue growth. Then, these droplets were transferred to a spinning bioreactor, resulting in the formation of

a complex tissue with discrete regions representing several different parts of the brain naturally developing in the organoids. This organoid model could be used not only to understand fundamental mechanisms of neurodevelopment, but also to study human brain development and disease. Hence, this model shows tremendous promise as a drug-screening model for brain disorders. Microfluidic devices could also be used to culture organoids under more well-controlled micro-environments.^[225] Au et al. developed a hepatic organoid culture model in a microfluidic device.^[226] Their microfluidic array enables many hepatic organoids to be formed simultaneously and spontaneously in microchambers. For such drug-screening studies, a high-throughput device must be engineered to save time and cost. In the future, the combination of brain organoids with a microfluidic device that is high throughput could open new doors for basic studies of neuronal development, in drug-screening as well as in tissue-engineering applications.

3.2. Neuromuscular Disorders-On-a-Chip

3.2.1. Motor Unit and NMJ

The NMJ might play a central role in the development of ALS causing atrophy of skeletal muscle fibers.^[227] NMJ differs from chemical synapses that link a motor neuron with a muscle fiber, which transmits the signal to muscle cells via acetylcholine receptors (AChR).^[228] During development, the signal from both the motor neuron terminal and muscle cell induces the formation of NMJ. First, muscle cells express distributed AChR on the surface of cells. After this, Agrin and MuSK kinase help the accumulation of AChR in the central region of the myocyte. Once motor neurons attach to myotubes and form an NMJ, ACh is released from the axonal terminals of motor neurons which positively reinforces the localization and stabilization of the developing NMJ.^[229] Acetylcholine released from neurons also regulates the efficacy of neurotransmission. For the contraction of muscle, the signaling from brain transmits a motor nerve action potential that reaches the presynaptic nerve terminal, eliciting release of a neurotransmitter (as also described in Section 2.3.3). This leads to an increase in intracellular calcium concentration by causing an increase in ion conductance, resulting in the fusion of the acetylcholine vesicles with the plasma membrane. Once acetylcholine is present in the synapse, it is able to bind to nicotinic acetylcholine receptors increasing the conductance of certain cations, sodium and potassium, in the postsynaptic membrane and producing an excitatory end plate current. Cations flowing into the postsynaptic cell cause a depolarization, as the membrane voltage increases above the normal resting potential. When the electrical signal exceeds a threshold magnitude, an action potential is generated post synoptically. This action potential propagates through the sarcolemma to the interior of the muscle fibers and eventually leads to an increase in intracellular calcium levels and subsequently initiating the process of excitation–contraction coupling. Once coupling begins, it allows the sarcomeres of the muscles to shorten, thus leading to the contraction of the muscle.^[230] This motor neuron–muscle communication is

vital for NMJ as well as for formation, maintenance, and proper functioning of skeletal muscle.

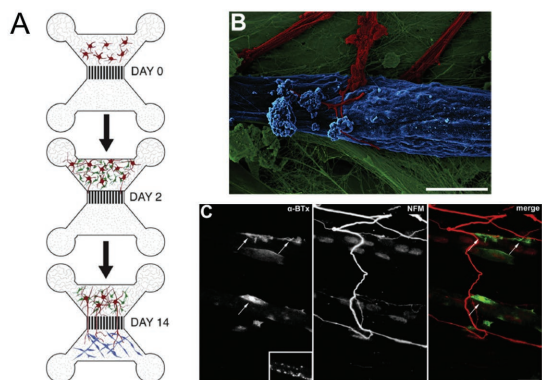
3.2.2. Amyotrophic Lateral Sclerosis

The most commonly known neurodegenerative disorder of motor neurons is ALS, which involves degeneration of both upper and lower motor neurons. This disease results from the proliferation of astrocytes caused by degeneration of the corticospinal tracts. ALS usually starts with painless weakening of the legs and arms and develops in one's 40s or 50s. To date, there are no effective treatments for sporadic ALS and familial ALS. Recent studies suggest that failure of the proteolysis pathway via autophagy affects development and progress of ALS.^[231–234] Nonetheless, the exact mechanism is unclear.

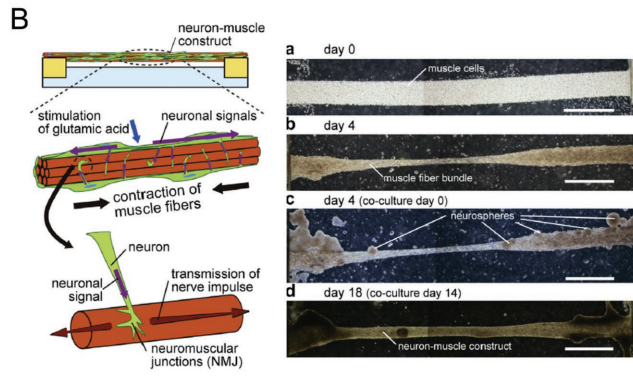
There are several different *in vitro* models to study ALS. Neurite elongation studies are used to investigate ALS as a model of new motor neuron innervation after injury in ALS patients. The most common way to analyze neurite elongation is monolayer culture on Petri dishes coated with poly-L-lysine (PLL) or poly-D-lysine (PDL) in a 2D culture system. However, we cannot control axon–dendrite polarity in 2D culture systems. In 1977, Campenot et al.^[235] developed a compartmented culture system consisting of a Teflon separator attached to a glass substrate, which allows for enhanced visualization of axon–dendrite polarity. In 2005, to improve on some of the limitations of this culture system, Taylor et al. proposed a PDMS-based compartmented high-throughput microfluidic device to study axon extension from neurons in brain and spinal cord (Figures 2H, 4B,C, and 5A). This culture platform was used to investigate axon regulation (proliferation, guidance, and extension)^[23] and to understand co-culture interactions with non-neuronal lineage cells.^[236] However, such a system has not yet been exploited for co-culture with spinal motor neuron–skeletal muscle cells, to form an NMJ and to test subsequent muscle contraction. In addition, Winkler et al. showed that blood–spinal cord barrier (BSCB) disruption leads to early motor neuron dysfunction and degeneration in an SOD-mutated ALS mouse model.^[237] Other groups have also claimed that both neuron–muscle cell interactions and neuron–endothelial cell interactions are important in forming blood–spinal cord barrier in ALS pathogenesis.^[238] Therefore, in engineering a new *in vitro* system that closely mimics ALS pathogenesis, we should reconstitute an integrated co-culture system using various types of cells (e.g., motor neurons, endothelial cells, Schwann cells, and skeletal muscle cells) to understand this complex mechanism.

Co-culture systems, including CMSs, form good NMJ models to potentially study ALS pathogenesis. Some of the first co-culture systems to study NMJ include early work by Southam et al. They demonstrated a novel *in vitro* model of lower motor neuromuscular junction circuit.^[239] They co-cultured motor neurons isolated from the spinal cords of embryonic rats and glial cells from the spinal cords of neonatal rats in one of the side compartments. After 14 d of culture, myotubes differentiated from myoblasts of neonatal rats were seeded in the other side-compartment. Elongated axons contacted the myotubes and formed neuromuscular junctions observed by

i) Formation of NMJ in 2D microfluidic chip



ii) Formation of NMJ in 3D cell culture



iii) Formation of Motor unit with NMJ in 3D microfluidic chip and optical stimulus

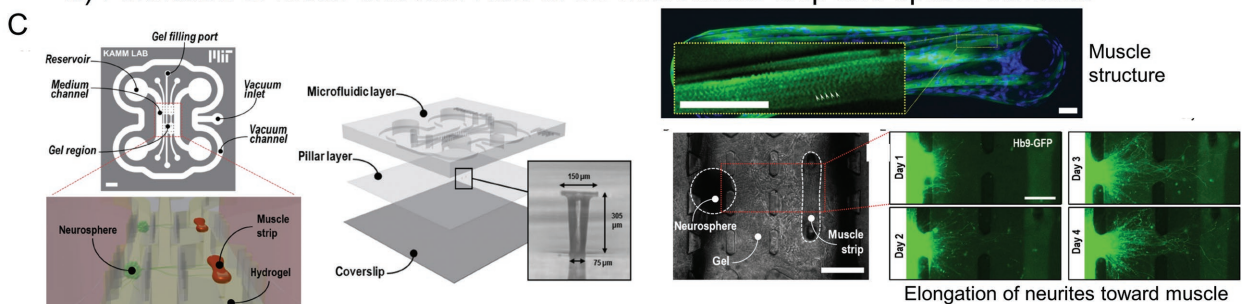


Figure 5. In vitro model of motor unit for neurodegenerative disease. A) Co-culture of skeletal muscle cells, motor neurons and astrocytes from the spinal cord of mouse embryo and fetal mouse. Motor neurons and astrocytes were cultured in the upper compartment, and skeletal myoblasts were cultured in lower compartment. Axons of motor neurons extend into lower compartment through the thin channels and reach the skeletal myotube resulting in formation of a neuromuscular junction. Reproduced with permission.^[239] 2013, Elsevier. B) In vitro formation of neuromuscular junctions with skeletal myotubes by culturing muscle cells in a narrow region patterned by Matrigel. Mouse-NSC-derived neurospheres directly attached to the muscle bundle and formed neuromuscular junctions with acetylcholine receptors (AChR). Reproduced with permission.^[240] 2016, Elsevier. C) An engineered motor unit with NMJ activated by optogenetics. A microfluidic device with three compartmentalized channels and pillar structures was developed. After formation of the C2C12 muscle bundle on pillar structures in one compartment, neurospheres genetically induced to express channelrhodopsin (ChR2) were injected into the left compartment. Axonal outgrowth toward the muscle bundle could be seen in 4 d, resulting in the formation of an NMJ. Optical stimulation of the neurospheres induced muscle bundle contraction indicating formation of a functional NMJ as well as maturation of the muscle bundle. Reproduced with permission.^[241] 2016, American Association for the Advancement of Science.

scanning electron microscopy (SEM) images (Figure 5A). They also showed that spinal glial cells and myotubes support motor neuron growth, indicating the necessity of the co-culture with some non-neuronal cells in order to mimic development of ALS in vitro. Ionescu et al. also showed a simplified and efficient system to demonstrate formation of NMJ in a compartmentalized microfluidic device.^[240] They also co-cultured mouse embryo-derived motor neurons and adult skeletal muscle cells in the device. Furthermore, various tests such as a muscle contraction assay, calcium transient recording, axonal growth, and imaging of the NMJ could be performed in the system to test proper functioning of the NMJ. Morimoto et al. developed a 3D neuron–muscular construct by culturing muscle cells in a narrow region patterned by Matrigel and mouse NSC-derived motor neurons on the muscular bundle (Figure 5B).^[242] They reported contraction in response to neurotransmitters released from neurons with synchronization. Each of these models demonstrates unique features in the development of drug-screening platforms for neurodegenerative disease involving NMJ dysfunction.

Some of the more recent work in NMJ disease models include optogenetically engineered cells to facilitate measurement of NMJ function (action potential stimulation, NMJ formation, and muscle contraction). For instance, Steinbeck et al. developed a simple 2D co-culture model using ChR2 motor neurons and human primary skeletal muscle cells to form the NMJ.^[243] To model neuromuscular disease, they added IgG from a myasthenia gravis patients, which is more biochemically reactive than control immunoglobulin G (IgG). They observed a reversible reduction in the amplitude of muscle contractions, representing a surrogate marker for the characteristic loss of muscle strength seen in myasthenia gravis. Recently, to improve upon models such as this, our group developed a compartmented microfluidic device with the reconstitution of 3D muscular strips and motor neuron elongation in 3D.^[241] C2C12 cells were seeded in one of the compartments with flexible pillar structures (Figure 5C), forming a muscular tissue strip anchored at the pillars with the capability of force measurement. Then, mouse-ESC-derived motor neuron spheres, optogenetically modified to express ChR2, were injected in a

neighboring compartment, and both compartments were filled with collagen hydrogel. This allowed the formation of neuronal elongation through the gel and subsequent formation of NMJs. Furthermore, optogenetic stimulation enabled contraction force in the microfluidic device to be measured in response to an intermittent light stimulus. Using this platform along with ALS-patient derived cells could potentially lead to a useful disease model.

3.2.3. Prospective Works for Neuromuscular Disorders-On-a-Chip

To date, studies of motor-unit-on-a-chip in CNS and PNS are focused primarily on investigating interactions between motor neurons and skeletal muscle cells. However, if we combine the state-of-the-art of current models and also incorporate neurovascular interactions, patient-derived cells (from iPSCs), optogenetics, microfluidics, and 3D printing technology, this would constitute a significant step forward in the development of *in vitro* neuromuscular disease models.

The motor neuron–vascular interactions or skeletal muscle–vascular interactions are important, yet largely ignored. This significance of the vascular tissues in neuromuscular disorders is likely due to their anatomical co-localization; in the CNS and PNS, neuronal networks and vascular networks are aligned in parallel with active cross-talk. Vascular networks support neuronal outgrowth and neuronal network development by efficient distribution of oxygen and nutrients.^[244] In addition, vascular networks play an important role in motor neuron degeneration. Garbuzova-Davis et al. found that the BSCB of endothelial cells breaks down followed by vascular alternation prior to motor neuron degeneration and neurovascular inflammation due to the loss of endothelial integrity in SOD1 mouse model as well as in ALS patients.^[238] The entry of blood-borne toxins could be an early key factor in ALS pathogenesis, resulting in motor neuron death. Furthermore, Winkler et al. found that red blood cells invading the tissue through the BSCB breakdown cause the generation of reactive oxygen species, inducing early motor neuron injury.^[237] Therefore, they proposed a strategy to prevent early motor neuron injury by blocking these injury steps using 5A-APC for BSCB repair as well as desferrioxamine (DFX) for iron chelation glutathione (GSH) for antioxidants. In addition to biochemical factors originating from blood, growth factors such as VEGF secreted from the surrounding vascular cells, also influence neuromuscular disorders. In healthy patients, sufficient expression of VEGF protein provides neuroprotection and oxygen supply to motor neurons. However, in ALS patients, a relatively low level of VEGF leads to compromised neuroprotection and perfusion resulting in motor neuron degeneration.^[245] By considering these mechanisms, Lambrechts et al. showed that VEGF treatment could protect against ischemic motor neuron death in an ALS mouse model. These findings revealed the therapeutic potential of VEGF for stressed motor neurons in human ALS patients.^[246] Although there are numerous studies reporting motor neuron degeneration, they are not sufficient to understand the entire pathogenesis of motor neuron degeneration. Further research is necessary in order to understand the interaction between vascular networks and motor neurons (as well as with skeletal myotubes).

Optogenetics is a key enabling technology. It could be used to test functional connectivity between motor neurons and skeletal muscle cells by optically activating specific ion channels. The transplantation of neuronal stem cells could be used therapeutically in neuroregeneration because it is difficult to regenerate nerves naturally. Stem cell grafts and electrochemical neuroprostheses may have potential use in the treatment of spinal cord injury. However, transplanted neurons cannot communicate with the rest of the nervous system. Bryson et al. showed optogenetic control of differentiated and transplanted motor neurons. In the mouse, activated motor neurons expressing ChR2 could re-establish connections within a damaged sciatic nerve system.^[247] This kind of optogenetic control of motor neurons could contribute to both the control of movement and repair of the nervous system. Optical stimulus training after motor neuron transplantation into zebrafish improves the repair of axons by increasing the level of cyclic adenosine monophosphate (cAMP).^[248] Optical stimulation could also be used to improve the contractile function in skeletal muscle (Figure 2L).^[249] Studies have already demonstrated the possibility of combining optogenetics and microfluidic devices to drive muscle contractions using localized optical stimulation (Figure 5C). This technique and further improvement and refinement of optogenetics (e.g., muscle training with optogenetics) could allow us to move to the next stage of investigations in neuronal and muscular activity.

3D printing could also be applied to aid basic cell biology studies, fabrication of microfluidic device, as well as applications in tissue engineering. Johnson et al. developed a bioinspired and customizable 3D-printed nervous system on a chip (3DNSC).^[250] This 3DNSC allows the assembly of a biomimetic scaffold for aligning neuronal axons and spatial organization of cells. 3DNSC consists of parallel microchannels, a sealant layer, and a third chamber was subsequently printed on top using silicone and grease. PNS neurons, Schwann cells, and the terminal cell junctions of the neurons were separately cultured in three different compartments, resulting in integrated neural networks. Such 3D-printing techniques improve the flexibility in the design of device architecture to create specific microenvironments.

To ultimately mimic ALS patient-specific conditions *in vitro*, it is necessary to use neuron and muscle cells from patient-derived iPSCs. Dimos et al. initially generated ALS patient-derived motor neurons from induced pluripotent stem cells.^[251] Son et al. introduced in 2011 a technique to start with mouse and human fibroblasts and eventually differentiate them to functional spinal motor neurons.^[252] Egawa et al. also established a technique to obtain ALS patient derived motor neurons from iPSC cells and examine the TDP43 protein.^[253] To further understand the mechanism of ALS, we need to combine these types of cells, recapitulate the microenvironment in microfluidic devices including an NMJ, and to eventually test the contraction force of muscle tissue fibers.

To apply motor unit and spinal-cord-on-a-chip platforms to screening for new drugs, it is necessary to use our biological insights from previous studies to fabricate novel *in vitro* systems. Such systems will use patient-derived cells efficiently differentiated from iPSCs along with state-of-the-art techniques in microfluidic device design (and 3D printing) to

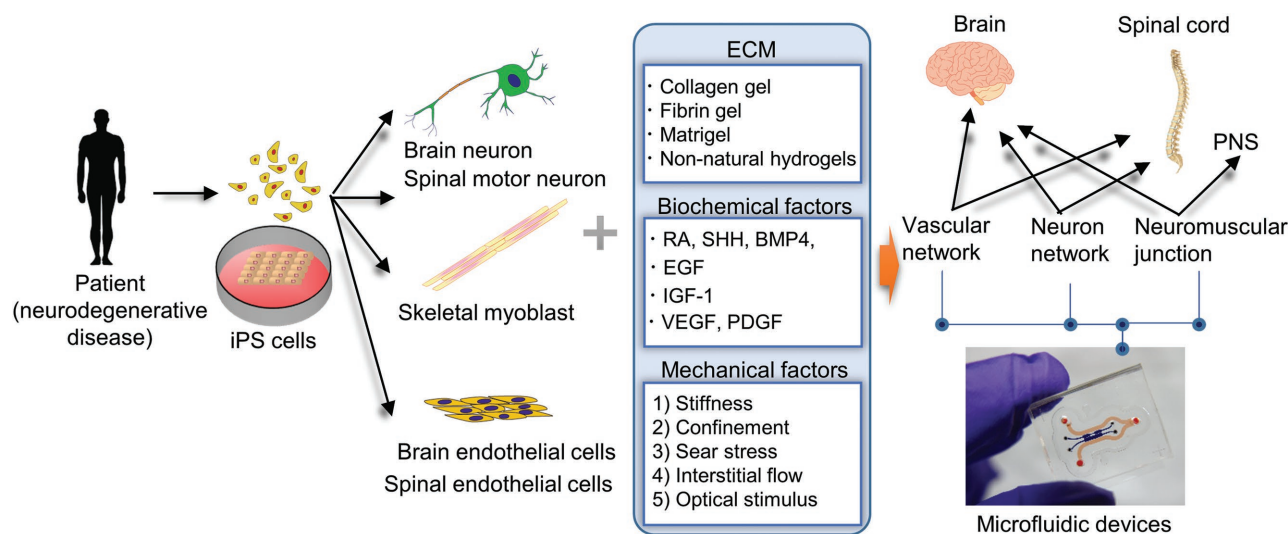


Figure 6. Prospective in vitro models for neurodegenerative disease. To more fully understand the mechanisms of pathogenesis in neurodegenerative diseases such as AD, PD, and motor neuron disorders (ALS), it is necessary to develop in vivo like in vitro systems. For this, we need to merge our biological knowledge (efficient differentiation methods, genetic modifications, and knockout mouse models) along with engineering techniques (microfluidic devices, bioreactors, and mechanical and optical stimulation) to meet specific requirements of organ- and disease-specific in vitro systems. In particular, the use of patient-derived iPS cells has tremendous potential for modeling specific disease, and has been shown to express the desired genotypes/phenotypes. Neurodegenerative diseases can be advanced by the integration of these patient-derived cells with microfluidic devices to mimic microenvironments, by the use of various ECMs, and by applying biochemical and mechanical factors. Combining vascular networks and neuronal networks into a neurovascular unit in brain or neuromuscular junctions is an important step toward mimicking the brain and spinal cord. Microfluidic devices have the capability to integrate these components into small lab-on-a-chip style devices with a range of applications.

reconstitute the microenvironment of the CNS and PNS. Also, mechanotransduction might play an important role in studying neuromuscular disorders due to the mechanically active microenvironment of NMJs.

4. Conclusion

This review gives an overview of applications of in vitro microfluidic device models in neurodegenerative diseases. The fundamental mechanisms giving rise to these diseases are still being identified and are unclear in many cases even though significant effort has been dedicated to this for decades. Reconstitution of in vivo like physiology and pathology in vitro could help in enhancing our understanding of disease pathogenesis as well as aid in drug discovery efforts.

In this review, we first summarized the advantages of microfluidic devices and described some of the existing models. Then, we discussed in detail the use of microfluidic devices to study the effect of biological and mechanical factors as well as methods to probe function of neural and vascular systems. We also mentioned specific in vitro models for brain-related disorders such as AD and PD and for diseases involving spinal cord and peripheral nerve disorders such as ALS with also mentioning their current drawbacks. Finally, we described prospective works for reconstitution of an in vitro neurodegenerative disease model. To fully understand the mechanism of pathogenesis of neurodegenerative diseases such as AD, PD, and motor neuron disorder (ALS), it is necessary to utilize expertise across a range of disciplines: merging our knowledge about biological processes such as efficient differentiation

methods, genetic engineering, knockout mouse models, and engineering techniques such as microfluidic devices, bioreactors, and mechanical and optical stimulation to meet specific requirements for an in vitro model (Figure 6). In particular, the use of patient-derived iPS cells has the potential to accelerate this field of research because many researchers have started to show that these patient-derived iPS cells express the genotype as well as phenotype of specific diseases. In the study of neurodegenerative diseases, the integration of these patient-derived cells with microfluidic devices to mimic the microenvironment using a variety of ECM biomaterials along with the applications of specific biochemical and mechanical factors could be the next frontier. Understanding how to engineer vascular networks and neuronal networks to form a neurovascular unit in brain along with neuromuscular junctions is important to mimic the brain and the spinal cord. Microfluidic devices now have the capability of integrating these components into small lab-on-a-chip style devices that could meet a variety of needs from basic science to translational drug discovery.

Acknowledgements

T.O. and Y.S. contributed equally to this work. T.O. was granted by Japan Society for the Promotion of Sciences (JSPS) as overseas research fellows. R.D.K., T.O., Y.J., and V.S. also acknowledge the support of National Science Foundation for a Science and Technology Center on Emergent Behaviors of Integrated Cellular Systems (CBET-0939511) and a grant from the Cure Alzheimer's Fund. V.S. would also like to acknowledge support from the SMART BioSym center. M.C. is supported by Ermenegildo Zegna Founder's Scholarship.

Conflict of Interest

The authors declare no conflict of interest.

Keywords

central nervous system, microfluidic devices, neurodegenerative diseases, neuromuscular junctions, organ-on-a-chip

Received: April 14, 2017

Revised: July 18, 2017

Published online: September 7, 2017

- [1] V. Jackson-Lewis, S. Przedborski, *Nat. Protoc.* **2007**, *2*, 141.
- [2] J. Blesa, S. Przedborski, *Front. Neuroanat.* **2014**, *8*, 155.
- [3] D. R. Rosen, T. Siddique, D. Patterson, D. A. Figlewicz, P. Sapp, A. Hentati, D. Donaldson, J. Goto, J. P. O'Regan, H. X. Deng, Z. Rahmani, A. Krizus, D. McKenna-Yasek, A. Cayabyab, S. M. Gaston, R. Berger, R. E. Tanzi, J. J. Halperin, B. Herzfeldt, R. Van den Bergh, W.-Y. Hung, T. Bird, G. Deng, D. W. Mulder, C. Smyth, N. G. Laing, E. Soriano, M. A. Pericak-Vance, J. Haines, G. A. Rouleau, J. S. Gusella, H. R. Horvitz, R. H. Brown jr., *Nature* **1993**, *362*, 59.
- [4] M. E. Gurney, H. Pu, A. Y. Chiu, M. C. Dal Canto, C. Y. Polchow, D. D. Alexander, J. Caliendo, A. Hentati, Y. W. Kwon, H. X. Deng, W. Chen, P. Zhai, R. L. Sufit, T. Siddique, *Science* **1994**, *264*, 1772.
- [5] W. M. S. Russell, *The Principles of Humane Experimental Technique* (Eds: W. M. S. Russell, R. L. Burch), Methuen, London, UK **1959**.
- [6] Y. Imamura, T. Mukohara, Y. Shimono, Y. Funakoshi, N. Chayahara, M. Toyoda, N. Kiyota, S. Takao, S. Kono, T. Nakatsura, H. Minami, *Oncol. Rep.* **2015**, *33*, 1837.
- [7] R. Edmondson, J. J. Broglie, A. F. Adcock, L. Yang, *Assay Drug Dev. Technol.* **2014**, *12*, 207.
- [8] H. Sawada, S. Shimohama, T. Kawamura, A. Akaike, Y. Kitamura, T. Taniguchi, J. Kimura, *J. Neurosci. Res.* **1996**, *46*, 509.
- [9] Y. Kitamura, T. Kosaka, J. I. Kakimura, Y. Matsuoka, Y. Kohno, Y. Nomura, T. Taniguchi, *Mol. Pharmacol.* **1998**, *54*, 1046.
- [10] J. H. Kim, J. M. Auerbach, J. A. Rodriguez-Gomez, I. Velasco, D. Gavin, N. Lumelsky, S. H. Lee, J. Nguyen, R. Sanchez-Pernaute, K. Bankiewicz, R. McKay, *Nature* **2002**, *418*, 50.
- [11] H. Sawada, M. Ibi, T. Kihara, K. Honda, T. Nakamizo, R. Kanki, M. Nakanishi, N. Sakka, A. Akaike, S. Shimohama, *Neuropharmacology* **2002**, *42*, 1056.
- [12] S. N. Bhatia, D. E. Ingber, *Nat. Biotechnol.* **2014**, *32*, 760.
- [13] K.-H. Nam, A. S. T. Smith, S. Lone, S. Kwon, D.-H. Kim, *J. Lab. Autom.* **2015**, *20*, 201.
- [14] a) J. El-Ali, P. K. Sorger, K. F. Jensen, *Nature* **2006**, *442*, 403; b) I. Meyvantsson, D. J. Beebe, *Annu. Rev. Anal. Chem.* **2008**, *1*, 423.
- [15] J. Zhang, K. Tan, G. Hong, L. Yang, H. Gong, *J. Micromech. Microeng.* **2001**, *11*, 20.
- [16] a) P. M. van Midwoud, A. Janse, M. T. Merema, G. M. Groothuis, E. Verpoorte, *Anal. Chem.* **2012**, *84*, 3938; b) J. Zhou, A. V. Ellis, N. H. Voelcker, *Electrophoresis* **2010**, *31*, 2.
- [17] a) N. L. Jeon, S. K. Dertinger, D. T. Chiu, I. S. Choi, A. D. Stroock, G. M. Whitesides, *Langmuir* **2000**, *16*, 8311; b) S. K. Dertinger, D. T. Chiu, N. L. Jeon, G. M. Whitesides, *Anal. Chem.* **2001**, *73*, 1240; c) V. V. Abhyankar, M. A. Lokuta, A. Huttenlocher, D. J. Beebe, *Lab Chip* **2006**, *6*, 389.
- [18] Z. Tong, E. M. Balzer, M. R. Dallas, W.-C. Hung, K. J. Stebe, K. Konstantopoulos, *PLoS One* **2012**, *7*, e29211.
- [19] a) G. M. Whitesides, A. D. Stroock, *Phys. Today* **2001**, *54*, 42; b) H. A. Stone, S. Kim, *AIChE J.* **2001**, *47*, 1250.
- [20] B. G. Chung, L. A. Flanagan, S. W. Rhee, P. H. Schwartz, A. P. Lee, E. S. Monuki, N. L. Jeon, *Lab Chip* **2005**, *5*, 401.
- [21] J. Y. Park, S. K. Kim, D. H. Woo, E. J. Lee, J. H. Kim, S. H. Lee, *Stem Cells* **2009**, *27*, 2646.
- [22] a) L. J. Millet, M. E. Stewart, R. G. Nuzzo, M. U. Gillette, *Lab Chip* **2010**, *10*, 1525; b) J. W. Park, B. Vahidi, A. M. Taylor, S. W. Rhee, N. L. Jeon, *Nat. Protoc.* **2006**, *1*, 2128.
- [23] A. M. Taylor, M. Blurton-Jones, S. W. Rhee, D. H. Cribbs, C. W. Cotman, N. L. Jeon, *Nat. Methods* **2005**, *2*, 599.
- [24] K. L. Butler, V. Ambraveswaran, N. Agrawal, M. Bilodeau, M. Toner, R. G. Tompkins, S. Fagan, D. Irimia, *PLoS One* **2010**, *5*, e11921.
- [25] S. M. Rao, V. K. Lin, U. Tata, G. V. Raj, J.-T. Hsieh, K. Nguyen, J.-C. Chiao, *J. Nanotechnol. Eng. Med.* **2010**, *1*, 021003.
- [26] X. J. Li, A. V. Valadez, P. Zuo, Z. Nie, *Bioanalysis.* **2012**, *4*, 1509.
- [27] Y. Shin, S. Han, J. S. Jeon, K. Yamamoto, I. K. Zervantonakis, R. Sudo, R. D. Kamm, S. Chung, *Nat. Protoc.* **2012**, *7*, 1247.
- [28] a) J. S. Jeon, S. Bersini, M. Gilardi, G. Dubini, J. L. Charest, M. Moretti, R. D. Kamm, *Proc. Natl. Acad. Sci. USA* **2015**, *112*, 214; b) M. B. Chen, J. A. Whisler, J. Fröse, C. Yu, Y. Shin, R. D. Kamm, *Nat. Protoc.* **2017**, *12*, 865; c) M. B. Chen, J. M. Lamar, R. Li, R. O. Hynes, R. D. Kamm, *Cancer Res.* **2016**, *76*, 2513.
- [29] Y. Shin, K. Yang, S. Han, H. J. Park, Y. Seok Heo, S. W. Cho, S. Chung, *Adv. Healthcare Mater.* **2014**, *3*, 1457.
- [30] K. Yang, H.-J. Park, S. Han, J. Lee, E. Ko, J. Kim, J. S. Lee, J. H. Yu, K. Y. Song, E. Cheong, *Biomaterials* **2015**, *63*, 177.
- [31] R. Sudo, S. Chung, I. K. Zervantonakis, V. Vickerman, Y. Toshimitsu, L. G. Griffith, R. D. Kamm, *FASEB J.* **2009**, *23*, 2155.
- [32] D. Huh, B. D. Matthews, A. Mammoto, M. Montoya-Zavala, H. Y. Hsin, D. E. Ingber, *Science* **2010**, *328*, 1662.
- [33] a) O. Frey, P. M. Misun, D. A. Fluri, J. G. Hengstler, A. Hierlemann, *Nat. Commun.* **2014**, *5*, 4250; b) P. M. Misun, J. Rothe, Y. R. Schmid, A. Hierlemann, O. Frey, *Microsyst. Nanoeng.* **2016**, *2*, 16022; c) X. Wang, S. Chen, Y. T. Chow, C.-w. Kong, R. A. Li, D. Sun, *RSC Adv.* **2013**, *3*, 23589; d) G. S. Jeong, Y. Jun, J. H. Song, S. H. Shin, S.-H. Lee, *Lab Chip* **2012**, *12*, 159.
- [34] A. M. Skelley, O. Kirak, H. Suh, R. Jaenisch, J. Voldman, *Nat. Methods* **2009**, *6*, 147.
- [35] K. K. Zeming, S. Ranjan, Y. Zhang, *Nat. Commun.* **2013**, *4*, 1625.
- [36] A. F. Sarioglu, N. Aceto, N. Kojic, M. C. Donaldson, M. Zeinali, B. Hamza, A. Engstrom, H. Zhu, T. K. Sundaresan, D. T. Miyamoto, X. Luo, A. Bardia, B. S. Wittner, S. Ramaswamy, T. Shioda, D. T. Ting, S. L. Stott, R. Kapur, S. Maheswaran, D. A. Haber, M. Toner, *Nat. Methods* **2015**, *12*, 685.
- [37] K. Takahashi, K. Tanabe, M. Ohnuki, M. Narita, T. Ichisaka, K. Tomoda, S. Yamanaka, *Cell* **2007**, *131*, 861.
- [38] S. I. Nishimura, M. Ueda, M. Sasai, *PLoS Comput. Biol.* **2009**, *5*, e1000310.
- [39] Q. Liu, C. Wu, H. Cai, N. Hu, J. Zhou, P. Wang, *Chem. Rev.* **2014**, *114*, 6423.
- [40] a) S. Herculano-Houzel, *Glia* **2014**, *62*, 1377; b) F. A. Azevedo, L. R. Carvalho, L. T. Grinberg, J. M. Farfel, R. E. Ferretti, R. E. Leite, R. Lent, S. Herculano-Houzel, *J. Comp. Neurol.* **2009**, *513*, 532; c) R. Lent, F. A. Azevedo, C. H. Andrade-Moraes, A. V. Pinto, *Eur. J. Neurosci.* **2012**, *35*, 1.
- [41] B. A. Barres, *Neuron* **2008**, *60*, 430.
- [42] R. D. Fields, D. H. Woo, P. J. Basser, *Neuron* **2015**, *86*, 374.
- [43] Y. Du, C. F. Dreyfus, *J. Neurosci. Res.* **2002**, *68*, 647.
- [44] a) L. Cheslow, J. I. Alvarez, *Curr. Opin. Pharmacol.* **2016**, *26*, 39; b) Y. Igarashi, H. Utsumi, H. Chiba, Y. Yamada-Sasamori, H. Tobioka, Y. Kamimura, K. Furuuchi, Y. Kokai, T. Nakagawa, M. Mori, *Biochem. Biophys. Res. Commun.* **1999**, *261*, 108.

- [45] J. P. Spanos, N.-J. Hsu, M. Jacobs, *Front. Cell. Neurosci.* **2015**, *9*, 182.
- [46] a) Y. Nakagawa, K. Chiba, *Pharmaceuticals* **2014**, *7*, 1028; b) M. Greter, I. Lelios, A. L. Croxford, *Front. Immunol.* **2015**, *6*, 249.
- [47] a) V. H. Perry, J. A. Nicoll, C. Holmes, *Nat. Rev. Neurol.* **2010**, *6*, 193; b) E. Solito, M. Sastre, *Front. Pharmacol.*, **2012**, *3*, 14.
- [48] N. J. Abbott, A. A. Patabendige, D. E. Dolman, S. R. Yusof, D. J. Begley, *Neurobiol. Dis.* **2010**, *37*, 13.
- [49] P. Ballabh, A. Braun, M. Nedergaard, *Neurobiol. Dis.* **2004**, *16*, 1.
- [50] E. A. Winkler, R. D. Bell, B. V. Zlokovic, *Nat. Neurosci.* **2011**, *14*, 1398.
- [51] A. Armulik, G. Genové, M. Mäe, M. H. Nisancioglu, E. Wallgard, C. Niaudet, L. He, J. Norlin, P. Lindblom, K. Strittmatter, *Nature* **2010**, *468*, 557.
- [52] J. Lok, P. Gupta, S. Guo, W. J. Kim, M. J. Whalen, K. van Leyen, E. H. Lo, *Neurochem. Res.* **2007**, *32*, 2032.
- [53] a) C. Hammond, *Cell. Mol. Neurophysiol.*, 4th. Elsevier: UK, **2014**. b) J. H. McCarty, *Assay Drug Dev. Technol.* **2005**, *3*, 89.
- [54] a) Y.-K. Choi, K.-W. Kim, *BMB Rep.* **2008**, *41*, 345; b) G. A. Garden, A. R. La Spada, *Neuron* **2012**, *73*, 886.
- [55] A. B. Salmina, *J. Alzheimer's Dis.* **2009**, *16*, 485.
- [56] R. D. Fields, B. Stevens-Graham, *Science* **2002**, *298*, 556.
- [57] a) M. Tajés, E. Ramos-Fernández, X. Weng-Jiang, M. Bosch-Morató, B. Guivernau, A. Eraso-Pichot, B. Salvador, X. Fernandez-Busquets, J. Roquer, F. J. Munoz, *Mol. Membr. Biol.* **2014**, *31*, 152; b) V. Muoio, P. Persson, M. Sendeski, *Acta Physiol.* **2014**, *210*, 790.
- [58] W. Cai, K. Zhang, P. Li, L. Zhu, J. Xu, B. Yang, X. Hu, Z. Lu, J. Chen, *Ageing Res. Rev.* **2016**, *34*, 77.
- [59] B. V. Zlokovic, *Nat. Rev. Neurosci.* **2011**, *12*, 723.
- [60] P. Ekman, R. Levenson, W. Friesen, *Science* **1983**, *221*, 1208.
- [61] M. Donaghy, *Motor Neuron Diseases*, John Wiley & Sons, Ltd, UK **2001**.
- [62] M. R. Deschenes, *Curr. Aging Sci.* **2011**, *4*, 209.
- [63] Z. W. Hall, J. R. Sanes, *Cell* **1993**, *72*, 99.
- [64] D. M. Fambrough, D. B. Drachman, S. Satyamurti, *Science* **1973**, *182*, 293.
- [65] E. F. Stanley, D. B. Drachman, *Brain Res.* **1983**, *261*, 172.
- [66] B. Lang, D. Wray, J. Newsom-Davis, A. Vincent, N. Murray, *Lancet* **1981**, *318*, 224.
- [67] L. G. Griffith, M. A. Swartz, *Nat. Rev. Mol. Cell Biol.* **2006**, *7*, 211.
- [68] a) S. Chung, R. Sudo, V. Vickerman, I. K. Zervantonakis, R. D. Kamm, *Ann. Biomed. Eng.* **2010**, *38*, 1164; b) F. Guo, J. B. French, P. Li, H. Zhao, C. Y. Chan, J. R. Fick, S. J. Benkovic, T. J. Huang, *Lab Chip* **2013**, *13*, 3152.
- [69] J. Park, H. Koito, J. Li, A. Han, *Biomed. Microdevices* **2009**, *11*, 1145.
- [70] K.-J. Jang, A. P. Mehr, G. A. Hamilton, L. A. McPartlin, S. Chung, K.-Y. Suh, D. E. Ingber, *Integr. Biol.* **2013**, *5*, 1119.
- [71] W. Liu, L. Li, X. Wang, L. Ren, X. Wang, J. Wang, Q. Tu, X. Huang, J. Wang, *Lab Chip* **2010**, *10*, 1717.
- [72] I. K. Zervantonakis, C. R. Kothapalli, S. Chung, R. Sudo, R. D. Kamm, *Biomicrofluidics* **2011**, *5*, 013406.
- [73] Y. Shin, J. S. Jeon, S. Han, G. S. Jung, S. Shin, S. H. Lee, R. Sudo, R. D. Kamm, S. Chung, *Lab Chip* **2011**, *11*, 2175.
- [74] C. Kim, J. Kasuya, J. Jeon, S. Chung, R. D. Kamm, *Lab Chip* **2015**, *15*, 301.
- [75] S. G. M. Uzel, O. C. Amadi, T. M. Pearl, R. T. Lee, P. T. C. So, R. D. Kamm, *Small* **2016**, *12*, 612.
- [76] T. A. Kapur, M. S. Shoichet, *J. Biomed. Mater. Res., Part A* **2004**, *68A*, 235.
- [77] C. R. Kothapalli, E. van Veen, S. de Valence, S. Chung, I. K. Zervantonakis, F. B. Gertler, R. D. Kamm, *Lab Chip* **2011**, *11*, 497.
- [78] H. G. Sundararaghavan, G. A. Monteiro, B. L. Firestein, D. I. Shreiber, *Biotechnol. Bioeng.* **2009**, *102*, 632.
- [79] J.-M. Peyrin, B. Deleglise, L. Saias, M. Vignes, P. Gougis, S. Magnifico, S. Betuing, M. Pietri, J. Caboche, P. Vanhoutte, J.-L. Viovy, B. Brugg, *Lab Chip* **2011**, *11*, 3663.
- [80] J. W. Song, L. L. Munn, *Proc. Natl. Acad. Sci. USA* **2011**, *108*, 15342.
- [81] S. Kim, H. Lee, M. Chung, N. L. Jeon, *Lab Chip* **2013**, *13*, 1489.
- [82] P. A. Galie, D. H. Nguyen, C. K. Choi, D. M. Cohen, P. A. Janmey, C. S. Chen, *Proc. Natl. Acad. Sci. USA* **2014**, *111*, 7968.
- [83] T. Asano, T. Ishizuka, K. Morishima, H. Yawo, *Sci. Rep.* **2015**, *5*, 8317.
- [84] C. P. Huang, J. Lu, H. Seon, A. P. Lee, L. A. Flanagan, H. Y. Kim, A. J. Putnam, N. L. Jeon, *Lab Chip* **2009**, *9*, 1740.
- [85] C. Nicholson, E. Sykova, *Trends Neurosci.* **1998**, *21*, 207.
- [86] E. Ruoslahti, *Glycobiology* **1996**, *6*, 489.
- [87] L. W. Lau, R. Cua, M. B. Keough, S. Haylock-Jacobs, V. W. Yong, *Nat. Rev. Neurosci.* **2013**, *14*, 722.
- [88] V. W. Yong, *Nat. Rev. Neurosci.* **2005**, *6*, 931.
- [89] C. Ricks, S. Shin, C. Becker, R. Grandhi, *Neural Regener. Res.* **2014**, *9*, 1573.
- [90] K. Chwalek, M. D. Tang-Schomer, F. G. Omenetto, D. L. Kaplan, *Nat. Protoc.* **2015**, *10*, 1362.
- [91] a) C. C. Tate, D. A. Shear, M. C. Tate, D. R. Archer, D. G. Stein, M. C. LaPlaca, *J. Tissue Eng. Regener. Med.* **2009**, *3*, 208; b) T. Oda, H. Taneichi, K. Takahashi, H. Togashi, M. Hangai, R. Nakagawa, M. Ono, M. Matsui, T. Sasai, K. Nagasawa, H. Honma, T. Kajiwara, Y. Takahashi, N. Takebe, Y. Ishigaki, J. Satoh, *Diabetic Med.* **2014**, *32*, 213.
- [92] a) S. Gnani, L. Blasio, C. Tonda-Turo, A. Mancardi, L. Primo, G. Ciardelli, G. Gambarotta, S. Geuna, I. Perroteau, *J. Tissue Eng. Regener. Med.* **2017**, *11*, 459; c) K. T. Morin, R. T. Tranquillo, *Exp. Cell Res.* **2013**, *319*, 2409.
- [93] a) W. Ma, W. Fitzgerald, Q.-Y. Liu, T. O'shaughnessy, D. Maric, H. Lin, D. Alkon, J. Barker, *Exp. Neurol.* **2004**, *190*, 276; b) S. M. Willerth, K. J. Arendas, D. I. Gottlieb, S. E. Sakiyama-Elbert, *Biomaterials* **2006**, *27*, 5990; c) J. Arulmoli, H. J. Wright, D. T. Phan, U. Sheth, R. A. Que, G. A. Botten, M. Keating, E. L. Botvinick, M. M. Pathak, T. I. Zarebinski, *Acta Biomater.* **2016**, *43*, 122; d) M. Antman-Passig, O. Shefi, *Nano Lett.* **2016**, *16*, 2567.
- [94] S. L. Madden, B. P. Cook, M. Nacht, W. D. Weber, M. R. Callahan, Y. Jiang, M. R. Dufault, X. Zhang, W. Zhang, J. Walter-Yohrling, *Am. J. Pathol.* **2004**, *165*, 601.
- [95] a) W. Tian, S. Hou, J. Ma, C. Zhang, Q. Xu, I. Lee, H. Li, M. Spector, F. Cui, *Tissue Eng.* **2005**, *11*, 513; b) Y. Wei, W. Tian, X. Yu, F. Cui, S. Hou, Q. Xu, I.-S. Lee, *Biomed. Mater.* **2007**, *2*, S142; c) Y. T. Wei, Y. He, C. L. Xu, Y. Wang, B. F. Liu, X. M. Wang, X. D. Sun, F. Z. Cui, Q. Y. Xu, *J. Biomed. Mater. Res., Part B* **2010**, *95*, 110.
- [96] Y. Wang, Y. T. Wei, Z. H. Zu, R. K. Ju, M. Y. Guo, X. M. Wang, Q. Y. Xu, F. Z. Cui, *Pharm. Res.* **2011**, *28*, 1406.
- [97] a) J. A. DeQuach, S. H. Yuan, L. S. Goldstein, K. L. Christman, *Tissue Eng., Part A* **2011**, *17*, 2583; b) S. Baiguera, C. Del Gaudio, E. Lucatelli, E. Kuevda, M. Boieri, B. Mazzanti, A. Bianco, P. Macchiarini, *Biomaterials* **2014**, *35*, 1205.
- [98] H.-W. Wang, X.-F. Lin, L.-R. Wang, Y.-Q. Lin, J.-T. Wang, W.-Y. Liu, G.-Q. Zhu, M. Braddock, M. Zhong, M.-H. Zheng, *Expert Rev. Neurother.* **2015**, *15*, 493.
- [99] a) C. Wang, X. Tong, F. Yang, *Mol. Pharm.* **2014**, *11*, 2115; b) M. J. Mahoney, K. S. Anseth, *J. Biomed. Mater. Res., Part A* **2007**, *81*, 269.
- [100] F. Yang, R. Murugan, S. Ramakrishna, X. Wang, Y.-X. Ma, S. Wang, *Biomaterials* **2004**, *25*, 1891.
- [101] M. A. Chernousov, W. M. Yu, Z. L. Chen, D. J. Carey, S. Strickland, *Glia* **2008**, *56*, 1498.
- [102] D. L. Sherman, C. Fabrizi, C. S. Gillespie, P. J. Brophy, *Neuron* **2001**, *30*, 677.

- [103] F. A. Court, D. L. Sherman, T. Pratt, E. M. Garry, R. R. Ribchester, D. F. Cottrell, S. M. Fleetwood-Walker, P. J. Brophy, *Nature* **2004**, 437, 191.
- [104] S. Rodin, A. Domogatskaya, S. Strom, E. M. Hansson, K. R. Chien, J. Inzunza, O. Hovatta, K. Tryggvason, *Nat. Biotechnol.* **2010**, 28, 611.
- [105] T. Miyazaki, S. Futaki, H. Suemori, Y. Taniguchi, M. Yamada, M. Kawasaki, M. Hayashi, H. Kumagai, N. Nakatsuji, K. Sekiguchi, E. Kawase, *Nat. Commun.* **2012**, 3, 1236.
- [106] D. Edgar, R. Timpl, H. Thoenen, *EMBO J.* **1984**, 3, 1463.
- [107] P. C. Buttery, C. French-Constant, *Mol. Cell. Neurosci.* **1999**, 14, 199.
- [108] S. Grefte, S. Vullings, A. M. Kuijpers-jagtman, R. Torensma, J. W. Von den Hoff, *Biomed. Mater.* **2012**, 7, 055004.
- [109] M. Uemura, M. M. Refaat, M. Shinoyama, H. Hayashi, N. Hashimoto, J. Takahashi, *J. Neurosci. Res.* **2010**, 88, 542.
- [110] G. Ramesh, M. T. Philipp, L. Vallières, A. G. MacLean, M. Ahmad, *Mediators Inflamm.* **2013**, 2013, 2.
- [111] T. Nagatsu, M. Mogi, H. Ichinose, A. Togari, Y. Mizuno, D. B. Calne, R. Horowski, W. Poewe, P. Riederer, M. B. H. Youdim, in *Advances in Research on Neurodegeneration*, Springer, Vienna, **2000**, p. 143.
- [112] H. Gerhardt, M. Golding, M. Fruttiger, C. Ruhrberg, A. Lundkvist, A. Abramsson, M. Jeltsch, C. Mitchell, K. Alitalo, D. Shima, C. Betsholtz, *J. Cell Biol.* **2003**, 161, 1163.
- [113] C. Hellberg, A. Ostman, C. H. Heldin, *Recent Results Cancer Res.* **2010**, 180, 103.
- [114] E. Pardali, M. J. Goumans, P. ten Dijke, *Trends Cell Biol.* **2010**, 20, 556.
- [115] A. Beenken, M. Mohammadi, *Nat. Rev. Drug Discovery* **2009**, 8, 235.
- [116] P. Carmeliet, R. K. Jain, *Nature* **2011**, 473, 298.
- [117] W. A. Farahat, L. B. Wood, I. K. Zervantonakis, A. Schor, S. Ong, D. Neal, R. D. Kamm, H. H. Asada, *PLoS One* **2012**, 7, e37333.
- [118] G. S. Jeong, S. Han, Y. Shin, G. H. Kwon, R. D. Kamm, S.-H. Lee, S. Chung, *Anal. Chem.* **2011**, 83, 8454.
- [119] B. L. Hogan, *Cell* **1999**, 96, 225.
- [120] J. B. Gurdon, P. Y. Bourillot, *Nature* **2001**, 413, 797.
- [121] B. N. Davis-Dusenbery, L. A. Williams, J. R. Klim, K. Eggan, *Development* **2014**, 141, 491.
- [122] W. A. Alaynick, T. M. Jessell, S. L. Pfaff, *Cell* **2011**, 146, 178.
- [123] C. J. Demers, P. Soundararajan, P. Chennampally, G. A. Cox, J. Briscoe, S. D. Collins, R. L. Smith, *Development* **2016**, 143, 1884.
- [124] P. C. Georges, W. J. Miller, D. F. Meaney, E. S. Sawyer, P. A. Janney, *Biophys. J.* **2006**, 90, 3012.
- [125] K. Hattori, Y. Munehira, H. Kobayashi, T. Satoh, S. Sugitara, T. Kanamori, *J. Biosci. Bioeng.* **2014**, 118, 327.
- [126] G. M. J. Beaudoin, S.-H. Lee, D. Singh, Y. Yuan, Y.-G. Ng, L. F. Reichardt, J. Arikath, *Nat. Protoc.* **2012**, 7, 1741.
- [127] M. W. Glynn, A. K. McAllister, *Nat. Protoc.* **2006**, 1, 1287.
- [128] L. González-Mariscal, A. Betanzos, P. Nava, B. E. Jaramillo, *Prog. Biophys. Mol. Biol.* **2003**, 81, 1.
- [129] M. N. Hart, L. F. VanDyk, S. A. Moore, D. M. Shasby, P. A. Cancilla, *J. Neuropathol. Exp. Neurol.* **1987**, 46, 141.
- [130] P. A. Vogel, S. T. Halpin, R. S. Martin, D. M. Spence, *Anal. Chem.* **2011**, 83, 4296.
- [131] G. Adriani, D. Ma, A. Pavesi, R. D. Kamm, E. L. K. Goh, *Lab Chip* **2017**, 17, 448.
- [132] A. Herland, A. D. van der Meer, E. A. FitzGerald, T.-E. Park, J. J. F. Sleeboom, D. E. Ingber, *PLoS One* **2016**, 11, e0150360.
- [133] K. Yamamizu, M. Iwasaki, H. Takakubo, T. Sakamoto, T. Ikuno, M. Miyoshi, T. Kondo, Y. Nakao, M. Nakagawa, H. Inoue, J. K. Yamashita, *Stem Cell Rep.* **2017**, 8, 634.
- [134] K. Carlsson, P. E. Danielsson, A. Liljeborg, L. Majlöf, R. Lenz, N. Åslund, *Opt. Lett.* **1985**, 10, 53.
- [135] S. Hayashi, Y. Okada, *Mol. Biol. Cell* **2015**, 26, 1743.
- [136] F. Helmchen, W. Denk, *Nat. Methods* **2005**, 2, 932.
- [137] M. L. Moya, Y.-H. Hsu, A. P. Lee, C. C. W. Hughes, S. C. George, *Tissue Eng., Part C* **2013**, 19, 730.
- [138] O. F. Khan, M. V. Sefton, *Biomed. Microdevices* **2011**, 13, 69.
- [139] U. Y. Schaff, M. M. Q. Xing, K. K. Lin, N. Pan, N. L. Jeon, S. I. Simon, *Lab Chip* **2007**, 7, 448.
- [140] N. Shirakigawa, T. Takei, H. Ijima, *J. Biosci. Bioeng.* **2013**, 116, 740.
- [141] D. S. Peterka, H. Takahashi, R. Yuste, *Neuron* **2011**, 69, 9.
- [142] A. Odawara, H. Katoh, N. Matsuda, I. Suzuki, *Sci. Rep.* **2016**, 6, 26181.
- [143] J. N. MacLean, R. Yuste, *Cold Spring Harb. Protoc.* **2009**, 2009, pdb prot5316.
- [144] J. Y. Lin, M. Z. Lin, P. Steinbach, R. Y. Tsien, *Biophys. J.* **2009**, 96, 1803.
- [145] O. Yizhar, L. E. Fenno, T. J. Davidson, M. Mogri, K. Deisseroth, *Neuron* **2011**, 71, 9.
- [146] R. Renault, N. Sukenik, S. Descroix, L. Malaquin, J.-L. Viovy, J.-M. Peyrin, S. Bottani, P. Monceau, E. Moses, M. Vignes, *PLoS One* **2015**, 10, e0120680.
- [147] H. Al-Ali, S. R. Beckerman, J. L. Bixby, V. P. Lemmon, *Exp. Neurol.* **2017**, 287, 423.
- [148] M. S. Cohen, C. B. Orth, H. J. Kim, N. L. Jeon, S. R. Jaffrey, *Proc. Natl. Acad. Sci. USA* **2011**, 108, 11246.
- [149] a) A. Coquinco, M. Cynader, *Microfluidic and Compartmentalized Platforms for Neurobiological Research*, Emilia Biffi, Humana Press, United States, Vol. 139, **2015**. b) E. Neto, L. Leitão, D. M. Sousa, C. J. Alves, I. S. Alencastre, P. Aguiar, M. Lamghari, *J. Neurosci.* **2016**, 36, 11573.
- [150] A. M. Taylor, D. C. Dieterich, H. T. Ito, S. A. Kim, E. M. Schuman, *Neuron* **2010**, 66, 57.
- [151] G. Robertson, T. J. Bushell, M. Zagnoni, *Integr. Biol.* **2014**, 6, 636.
- [152] I. H. Yang, D. Gary, M. Malone, S. Dria, T. Houdayer, V. Belegu, J. W. McDonald, N. Thakor, *Neuromol. Med.* **2012**, 14, 112.
- [153] P. Pagella, E. Neto, M. Lamghari, T. A. Mitsiadis, *Eur. Cell. Mater.* **2015**, 29, 213.
- [154] E. Neto, C. J. Alves, D. M. Sousa, I. S. Alencastre, A. H. Lourenço, L. Leitão, H. R. Ryu, N. L. Jeon, R. Fernandes, P. Aguiar, *Integr. Biol.* **2014**, 6, 586.
- [155] A. Takeuchi, K. Shimba, M. Mori, Y. Takayama, H. Moriguchi, K. Kotani, J.-K. Lee, M. Noshiro, Y. Jimbo, *Integr. Biol.* **2012**, 4, 1532.
- [156] A. Kunze, S. Lengacher, E. Dirren, P. Aebischer, P. J. Magistretti, P. Renaud, *Integr. Biol.* **2013**, 5, 964.
- [157] J. M. Jang, J. Lee, H. Kim, N. L. Jeon, W. Jung, *Lab Chip* **2016**, 16, 1684.
- [158] J. M. Jang, S.-H.-T. Tran, S. C. Na, N. L. Jeon, *ACS Appl. Mater. Interfaces* **2015**, 7, 2183.
- [159] S. Bang, S. Na, J. M. Jang, J. Kim, N. L. Jeon, *Adv. Healthcare Mater.* **2015**, 5, 159.
- [160] P. Vulto, S. Podszun, P. Meyer, C. Hermann, A. Manz, G. A. Urban, *Lab Chip* **2011**, 11, 1596.
- [161] N. R. Wevers, R. van Vught, K. J. Wilschut, A. Nicolas, C. Chiang, H. L. Lanz, S. J. Trietsch, J. Joore, P. Vulto, *Sci. Rep.* **2016**, 6, 38856.
- [162] A. Kunze, M. Giugliano, A. Valero, P. Renaud, *Biomaterials* **2011**, 32, 2088.
- [163] a) T. Yagi, D. Ito, Y. Okada, W. Akamatsu, Y. Nihei, T. Yoshizaki, S. Yamanaka, H. Okano, N. Suzuki, *Hum. Mol. Genet.* **2011**, 20, 4530; b) J. Sandoe, K. Eggan, *Nat. Neurosci.* **2013**, 16, 780.
- [164] a) S. H. Choi, Y. H. Kim, M. Hebisch, C. Sliwinski, S. Lee, C. D'Avanzo, H. Chen, B. Hooli, C. Asselin, J. Muffat, *Nature* **2014**, 515, 274; b) Y. H. Kim, S. H. Choi, C. D'Avanzo, M. Hebisch, C. Sliwinski, E. Bylykbashi, K. J. Washicosky, J. B. Klee, O. Brüstle, R. E. Tanzi, *Nat. Protoc.* **2015**, 10, 985.
- [165] M. P. Lutolf, H. M. Blau, *Adv. Mater.* **2009**, 21, 3255.

- [166] E. W. Young, D. J. Beebe, *Chem. Soc. Rev.* **2010**, *39*, 1036.
- [167] a) H. Xu, S. C. Heilshorn, *Small* **2013**, *9*, 585; b) S. Cosson, M. Lutolf, *Sci. Rep.* **2014**, *4*, 4462.
- [168] a) L. G. Villa-Diaz, Y.-s. Torisawa, T. Uchida, J. Ding, N. C. Nogueira-de-Souza, K. S. O'shea, S. Takayama, G. D. Smith, *Lab Chip* **2009**, *9*, 1749; b) W.-T. Fung, A. Beyzavi, P. Abgrall, N.-T. Nguyen, H.-Y. Li, *Lab Chip* **2009**, *9*, 2591.
- [169] S. Han, K. Yang, Y. Shin, J. S. Lee, R. D. Kamm, S. Chung, S.-W. Cho, *Lab Chip* **2012**, *12*, 2305.
- [170] Z. Hesari, M. Soleimani, F. Atyabi, M. Sharifdini, S. Nadri, M. E. Warkiani, M. Zare, R. Dinarvand, *J. Biomed. Mater. Res., Part A* **2016**, *104*, 1534.
- [171] R. Daneman, L. Zhou, A. A. Kebede, B. A. Barres, *Nature* **2010**, *468*, 562.
- [172] a) R. Kortekaas, K. L. Leenders, J. C. van Oostrom, W. Vaalburg, J. Bart, A. Willemsen, N. H. Hendrikse, *Ann. Neurol.* **2005**, *57*, 176; b) J. Drouin-Ouellet, S. J. Sawiak, G. Cisbani, M. Lagacé, W. L. Kuan, M. Saint-Pierre, R. J. Dury, W. Alata, I. St-Amour, S. L. Mason, *Ann. Neurol.* **2015**, *78*, 160.
- [173] V. Berezowski, C. Landry, S. Lundquist, L. Dehouck, R. Cecchelli, M. P. Dehouck, L. Fenart, *Pharm. Res.* **2004**, *21*, 756.
- [174] Y. I. Wang, H. E. Abaci, M. L. Shuler, *Biotechnol. Bioeng.* **2017**, *114*, 184.
- [175] H. Cho, J. H. Seo, K. K. Wong, Y. Terasaki, J. Park, K. Bong, K. Arai, E. H. Lo, D. Irimia, *Sci. Rep.* **2015**, *5*, 15222.
- [176] S. P. Deosarkar, B. Prabhakarandian, B. Wang, J. B. Sheffield, B. Krynska, M. F. Kiani, *PLoS One* **2015**, *10*, e0142725.
- [177] J. D. Wang, E.-S. Khafagy, K. Khanafer, S. Takayama, M. E. ElSayed, *Mol. Pharm.* **2016**, *13*, 895.
- [178] J. A. Brown, V. Pensabene, D. A. Markov, V. Allwardt, M. D. Neely, M. Shi, C. M. Britt, O. S. Hoilett, Q. Yang, B. M. Brewer, P. C. Samson, L. J. McCawley, J. M. May, D. J. Webb, D. Li, A. B. Bowman, R. S. Reiserer, J. P. Wikswow, *Biomicrofluidics*. **2015**, *9*, 054124.
- [179] J. A. Kim, H. N. Kim, S.-K. Im, S. Chung, J. Y. Kang, N. Choi, *Biomicrofluidics* **2015**, *9*, 024115.
- [180] R. Booth, H. Kim, *Lab Chip* **2012**, *12*, 1784.
- [181] L. Griep, F. Wolbers, B. De Wagenaar, P. Ter Braak, B. Weksler, I. A. Romero, P. Couraud, I. Vermes, A. Van Der Meer, A. Van den Berg, *Biomed. Microdevices* **2013**, *15*, 145.
- [182] P. P. Partyka, G. A. Godsey, J. R. Galie, M. C. Kosciuk, N. K. Acharya, R. G. Nagele, P. A. Galie, *Biomaterials* **2017**, *115*, 30.
- [183] B. Prabhakarandian, M. C. Shen, J. B. Nichols, I. R. Mills, M. Sidoryk-Wegrzynowicz, M. Aschner, K. Pant, *Lab Chip* **2013**, *13*, 1093.
- [184] A. K. H. Achyuta, A. J. Conway, R. B. Crouse, E. C. Bannister, R. N. Lee, C. P. Katnik, A. A. Behensky, J. Cuevas, S. S. Sundaram, *Lab Chip* **2013**, *13*, 542.
- [185] J. H. Yeon, D. Na, K. Choi, S. W. Ryu, C. Choi, J. K. Park, *Biomed. Microdevices* **2012**, *14*, 1141.
- [186] F. R. Walter, S. Valkai, A. Kincses, A. Petneházi, T. Czeller, S. Veszélka, P. Ormos, M. A. Deli, A. Dér, *Sens. Actuators, B* **2016**, *222*, 1209.
- [187] K. L. Sellgren, B. T. Hawkins, S. Grego, *Biomicrofluidics*. **2015**, *9*, 061102.
- [188] J. Labus, S. Häckel, L. Lucka, K. Danker, *J. Neurosci. Methods*. **2014**, *228*, 35.
- [189] L. B. Thomsen, A. Burkhart, T. Moos, *PloS One* **2015**, *10*, e0134765.
- [190] S. Nakagawa, M. A. Deli, H. Kawaguchi, T. Shimizudani, T. Shimono, Á. Kittel, K. Tanaka, M. Niwa, *Neurochem. Int.* **2009**, *54*, 253.
- [191] S. F. Merkel, A. M. Andrews, E. M. Lutton, D. Mu, E. Hudry, B. T. Hyman, C. A. Maguire, S. H. Ramirez, *J. Neurochem.* **2017**, *140*, 216.
- [192] Y. I. Wang, H. E. Abaci, M. L. Shuler, *Biotechnol. Bioeng.* **2017**, *114*, 184.
- [193] a) L. L. Bischel, E. W. K. Young, B. R. Mader, D. J. Beebe, *Biomaterials* **2013**, *34*, 1471; b) G. M. Walker, D. J. Beebe, *Lab Chip* **2002**, *2*, 131.
- [194] B.-G. Xiao, C.-Z. Lu, H. Link, *J. Cell. Mol. Med.* **2007**, *11*, 1272.
- [195] S. S. Choi, H. J. Lee, I. Lim, J.-i. Satoh, S. U. Kim, *PLoS One* **2014**, *9*, e92325.
- [196] K. Zsebo, V. Yuschenkoff, S. Schiffer, D. Chang, E. McCall, C. Dinarello, M. Brown, B. Altmann, G. J. Bagby, *Blood* **1988**, *71*, 99.
- [197] A. Schneider, C. Krüger, T. Steigleder, D. Weber, C. Pitzer, R. Laage, J. Aronowski, M. H. Maurer, N. Gassler, W. Mier, M. Hasselblatt, R. Kollmar, S. Schwab, C. Sommer, A. Bach, H.-G. Kuhn, W. R. Schäbitz, *J. Clin. Invest.* **2005**, *115*, 2083.
- [198] J. Hardy, D. J. Selkoe, *Science* **2002**, *297*, 353.
- [199] a) S. A. Grathwohl, R. E. Kälin, T. Bolmont, S. Prokop, G. Winkelmann, S. A. Kaeser, J. Odenthal, R. Radde, T. Eldh, S. Gandy, *Nat. Neurosci.* **2009**, *12*, 1361; b) J. M. Rubio-Perez, J. M. Morillas-Ruiz, *Sci. World J.* **2012**, *2012*, 756357.
- [200] P. Joshi, E. Turola, A. Ruiz, A. Bergami, D. D. Libera, L. Benussi, P. Giussani, G. Magnani, G. Comi, G. Legname, *Cell Death Differ.* **2014**, *21*, 582.
- [201] M. Eufemi, R. Cocchiola, D. Romaniello, V. Correani, L. Di Francesco, C. Fabrizi, B. Maras, M. E. Schininà, *Neurochem. Int.* **2015**, *81*, 48.
- [202] P. Naik, L. Cucullo, *J. Pharm. Sci.* **2012**, *101*, 1337.
- [203] Y. J. Choi, S. Chae, J. H. Kim, K. F. Barald, J. Y. Park, S.-H. Lee, *Sci. Rep.* **2013**, *3*, 1921.
- [204] J. Park, B. K. Lee, G. S. Jeong, J. K. Hyun, C. J. Lee, S.-H. Lee, *Lab Chip* **2015**, *15*, 141.
- [205] B. Deleglise, S. Magnifico, E. Duplus, P. Vaur, V. Soubeyre, M. Belle, M. Vignes, J.-L. Viovy, E. Jacotot, J.-M. Peyrin, *Acta Neuropathol. Commun.* **2014**, *2*, 145.
- [206] H. L. Song, S. Shim, D. H. Kim, S. H. Won, S. Joo, S. Kim, N. L. Jeon, S. Y. Yoon, *Ann. Neurol.* **2014**, *75*, 88.
- [207] a) S. Takeda, S. Wegmann, H. Cho, S. L. DeVos, C. Commins, A. D. Roe, S. B. Nicholls, G. A. Carlson, R. Pitstick, C. K. Nobuhara, *Nat. Commun.* **2015**, *6*, 8490; b) S. Dujardin, K. Lécolle, R. Caillierez, S. Bégard, N. Zommer, C. Lachaud, S. Carrier, N. Dufour, G. Aurégan, J. Winderickx, *Acta Neuropathol. Commun.* **2014**, *2*, 14.
- [208] H. Cho, T. Hashimoto, E. Wong, Y. Hori, L. B. Wood, L. Zhao, K. M. Haigis, B. T. Hyman, D. Irimia, *Sci. Rep.* **2013**, *3*, 1823.
- [209] F. Bianco, N. Tonna, R. D. Lovchik, R. Mastrangelo, R. Morini, A. Ruiz, E. Delamarche, M. Matteoli, *Anal. Chem.* **2012**, *84*, 9833.
- [210] A. J. Lees, *Neurology* **2009**, *72*, S2.
- [211] J. Lotharius, P. Brundin, *Nat. Rev. Neurosci.* **2002**, *3*, 932.
- [212] K. A. Conway, J. D. Harper, P. T. Lansbury, *Nat. Med.* **1998**, *4*, 1318.
- [213] C. W. Olanow, P. Brundin, *Mov. Disord.* **2013**, *28*, 31.
- [214] E. C. Freundt, N. Maynard, E. K. Clancy, S. Roy, L. Bousset, Y. Sourigues, M. Covert, R. Melki, K. Kirkegaard, M. Brahic, *Ann. Neurol.* **2012**, *72*, 517.
- [215] J. M. Gil, A. C. Rego, *Eur. J. Neurosci.* **2008**, *27*, 2803.
- [216] M. A. Hickey, M.-F. Chesselet, *Prog. Neuro-Psychopharmacol. Biol. Psychiatry* **2003**, *27*, 255.
- [217] E. Cattaneo, C. Zuccato, M. Tartari, *Nat. Rev. Neurosci.* **2005**, *6*, 919.
- [218] J.-H. J. Cha, *Prog. Neurobiol.* **2007**, *83*, 228.
- [219] J. Bradford, J. Y. Shin, M. Roberts, C. E. Wang, G. Sheng, S. Li, X. J. Li, *J. Biol. Chem.* **2010**, *285*, 10653.
- [220] The HD iPSC Consortium, *Cell Stem Cell* **2012**, *11*, 264.
- [221] I.-H. Park, N. Arora, H. Huo, N. Maherali, T. Ahfeldt, A. Shimamura, M. W. Lensch, C. Cowan, K. Hochedlinger, G. Q. Daley, *Cell* **2008**, *134*, 877.

- [222] S. Camnasio, A. D. Carri, A. Lombardo, I. Grad, C. Mariotti, A. Castucci, B. Rozell, P. L. Riso, V. Castiglioni, C. Zuccato, C. Rochon, Y. Takashima, G. Diaferia, I. Biunno, C. Gellera, M. Jacconi, A. Smith, O. Hovatta, L. Naldini, S. Di Donato, A. Feki, E. Cattaneo, *Neurobiol. Dis.* **2012**, *46*, 41.
- [223] J. D. Miller, Y. M. Ganat, S. Kishinevsky, R. L. Bowman, B. Liu, E. Y. Tu, P. K. Mandal, E. Vera, J.-w. Shim, S. Kriks, T. Taldone, N. Fusaki, M. J. Tomishima, D. Krainc, T. A. Milner, D. J. Rossi, L. Studer, *Cell Stem Cell*, **2013**, *13*, 691.
- [224] M. A. Lancaster, M. Renner, C.-A. Martin, D. Wenzel, L. S. Bicknell, M. E. Hurler, T. Homfray, J. M. Penninger, A. P. Jackson, J. A. Knoblich, *Nature* **2013**, *501*, 373.
- [225] A. Skardal, T. Shupe, A. Atala, *Drug Discovery Today* **2016**, *21*, 1399.
- [226] S. H. Au, M. D. Chamberlain, S. Mahesh, M. V. Sefton, A. R. Wheeler, *Lab Chip* **2014**, *14*, 3290.
- [227] J. E. Heuser, T. S. Reese, *J. Cell Biol.* **1973**, *57*, 315.
- [228] M. H. Wilson, M. R. Deschenes, *Int. J. Neurosci.* **2005**, *115*, 803.
- [229] K. Okada, A. Inoue, M. Okada, Y. Murata, S. Kakuta, T. Jigami, S. Kubo, H. Shiraishi, K. Eguchi, M. Motomura, T. Akiyama, Y. Iwakura, O. Higuchi, Y. Yamanashi, *Science* **2006**, *312*, 1802.
- [230] S. M. Sine, *Physiol. Rev.* **2012**, *92*, 1189.
- [231] N. Mizushima, T. Yoshimori, Y. Ohsumi, *Annu. Rev. Cell Dev. Biol.* **2011**, *27*, 107.
- [232] Q. J. Wang, Y. Ding, D. S. Kohtz, N. Mizushima, I. M. Cristea, M. P. Rout, B. T. Chait, Y. Zhong, N. Heintz, Z. Yue, *J. Neurosci.* **2006**, *26*, 8057.
- [233] F. Navone, P. Genevini, N. Borgese, *Cells* **2015**, *4*, 354.
- [234] A. Otomo, L. Pan, S. Hadano, *Neurol. Res. Int.* **2012**, *2012*, 498428.
- [235] R. B. Campenot, *Proc. Natl. Acad. Sci. USA* **1977**, *74*, 4516.
- [236] J. Park, H. Koito, J. Li, A. Han, *Biomed. Microdevices* **2009**, *11*, 1145.
- [237] E. A. Winkler, J. D. Sengillo, A. P. Sagare, Z. Zhao, Q. Ma, E. Zuniga, Y. Wang, Z. Zhong, J. S. Sullivan, J. H. Griffin, D. W. Cleveland, B. V. Zlokovic, *Proc. Natl. Acad. Sci. USA* **2014**, *111*, E1035.
- [238] S. Garbuzova-Davis, D. G. Hernandez-Ontiveros, M. C. Rodrigues, E. Haller, A. Frisina-Deyo, S. Mirtyl, S. Sallot, S. Saporta, C. V. Borlongan, P. R. Sanberg, *Brain Res.* **2012**, *1469*, 114.
- [239] K. A. Southam, A. E. King, C. A. Blizzard, G. H. McCormack, T. C. Dickson, *J. Neurosci. Methods* **2013**, *218*, 164.
- [240] A. Ionescu, E. E. Zahavi, T. Gradus, K. Ben-Yaakov, E. Perlson, *Eur. J. Cell Biol.* **2016**, *95*, 69.
- [241] S. G. Uzel, R. J. Platt, V. Subramanian, T. M. Pearl, C. J. Rowlands, V. Chan, L. A. Boyer, P. T. So, R. D. Kamm, *Sci. Adv.* **2016**, *2*, e1501429.
- [242] Y. Morimoto, M. Kato-Negishi, H. Onoe, S. Takeuchi, *Biomaterials* **2013**, *34*, 9413.
- [243] J. A. Steinbeck, M. K. Jaiswal, E. L. Calder, S. Kishinevsky, A. Weishaupt, K. V. Toyka, P. A. Goldstein, L. Studer, *Cell Stem Cell* **2016**, *18*, 134.
- [244] P. Carmeliet, *Nat. Rev. Genet.* **2003**, *4*, 710.
- [245] E. Storkebaum, A. Quaegebeur, M. Viskula, P. Carmeliet, *Nat. Neurosci.* **2011**, *14*, 1390.
- [246] D. Lambrechts, E. Storkebaum, M. Morimoto, J. Del-Favero, F. Desmet, S. L. Marklund, S. Wyns, V. Thijs, J. Andersson, I. van Marion, A. Al-Chalabi, S. Bornes, R. Musson, V. Hansen, L. Beckman, R. Adolfsson, H. S. Pall, H. Prats, S. Vermeire, P. Rutgeerts, S. Katayama, T. Awata, N. Leigh, L. Lang-Lazdunski, M. Dewerchin, C. Shaw, L. Moons, R. Vlietinck, K. E. Morrison, W. Robberecht, C. Van Broeckhoven, D. Collen, P. M. Andersen, P. Carmeliet, *Nat. Genet.* **2003**, *34*, 383.
- [247] J. B. Bryson, C. B. Machado, M. Crossley, D. Stevenson, V. Bros-Facer, J. Burrone, L. Greensmith, I. Lieberam, *Science* **2014**, *344*, 94.
- [248] Y. Xiao, W. Tian, H. López-Schier, *Curr. Biol.* **25**, R1068.
- [249] T. Bruegmann, T. van Bremen, C. C. Vogt, T. Send, B. K. Fleischmann, P. Sasse, *Nat. Commun.* **2015**, *6*, 7153.
- [250] B. N. Johnson, K. Z. Lancaster, I. B. Hogue, F. Meng, Y. L. Kong, L. W. Enquist, M. C. McAlpine, *Lab Chip* **2016**, *16*, 1393.
- [251] J. T. Dimos, K. T. Rodolfa, K. K. Niakan, L. M. Weisenthal, H. Mitumoto, W. Chung, G. F. Croft, G. Saphier, R. Leibel, R. Goland, H. Wichterle, C. E. Henderson, K. Eggan, *Science* **2008**, *321*, 1218.
- [252] E. Y. Son, J. K. Ichida, B. J. Wainger, J. S. Toma, V. F. Rafuse, C. J. Woolf, K. Eggan, *Cell Stem Cell* **2011**, *9*, 205.
- [253] N. Egawa, S. Kitaoka, K. Tsukita, M. Naitoh, K. Takahashi, T. Yamamoto, F. Adachi, T. Kondo, K. Okita, I. Asaka, T. Aoi, A. Watanabe, Y. Yamada, A. Morizane, J. Takahashi, T. Ayaki, H. Ito, K. Yoshikawa, S. Yamawaki, S. Suzuki, D. Watanabe, H. Hioki, T. Kaneko, K. Makioka, K. Okamoto, H. Takuma, A. Tamaoka, K. Hasegawa, T. Nonaka, M. Hasegawa, A. Kawata, M. Yoshida, T. Nakahata, R. Takahashi, M. C. N. Marchetto, F. H. Gage, S. Yamanaka, H. Inoue, *Sci. Transl. Med.* **2012**, *4*, 145ra104.